Developmental and Comparative Immunology 162 (2025) 105283

Contents lists available at ScienceDirect

Developmental and Comparative Immunology

journal homepage: www.elsevier.com/locate/devcompimm

Molecular depiction and functional delineation of E3 ubiquitin ligase MARCH5 in yellowtail clownfish (*Amphiprion clarkii*)

B.P.M. Vileka Jayamali [a], H.M.S.M. Wijerathna [a], D.M.K.P. Sirisena [a], H.A.C.R. Hanchapola [a], W.A.D.L.R. Warnakula [a], U.P.E. Arachchi [a], D.S. Liyanage [a], Sumi Jung [a,b], Qiang Wan [a,b,**], Jehee Lee [a,b,*]

[a] Department of Marine Life Sciences & Center for Genomic Selection in Korean Aquaculture, Jeju National University, Jeju, 63243, Republic of Korea
[b] Marine Life Research Institute, Kidang Marine Science Institute of Jeju National University, Jeju Self-Governing Province, 63333, Republic of Korea

ARTICLE INFO

Keywords:
MARCH5
Viral replication
Cytokine expression
Anti-apoptotic
Innate immunity

ABSTRACT

Membrane-associated Ring-CH 5 (MARCH5) is a mitochondrial E3 ubiquitin ligase playing a key role in the regulation of mitochondrial dynamics. In mammals, MARCH5 negatively regulates mitochondrial antiviral signaling (MAVS) protein aggregation during viral infection and hampers downstream type I interferon signaling to prevent excessive immune activation. However, its precise functional role in the teleost immune system remains unclear. This study investigated the molecular characteristics and immune response of the MARCH5 ortholog in *Amphiprion clarkii* (*A. clarkii*; AcMARCH5). The predicted AcMARCH5 protein sequence consists of 287 amino acids with a molecular weight of 32.02 kDa and a theoretical isoelectric point of 9.11. It contains four C-terminal transmembrane (TM) domains and an N-terminal RING cysteine-histidine (CH) domain, which directly regulates ubiquitin transfer. Multiple sequence alignment revealed a high level of conservation between AcMARCH5 and its orthologs in other vertebrate species. Under normal physiological conditions, *AcMARCH5* showed the highest mRNA expression in the muscle, brain, and kidney tissues of *A. clarkii*. Upon stimulation with polyinosinic:polycytidylic acid (Poly I:C), lipopolysaccharide (LPS), and *Vibrio harveyi*, *AcMARCH5* expression was drastically modulated. Functional assays showed that overexpression of AcMARCH5 in fathead minnow (FHM) cells downregulated antiviral gene expression, accompanied by enhanced viral hemorrhagic septicemia virus (VHSV) replication. In murine macrophages, AcMARCH5 overexpression markedly reduced the production of pro-inflammatory cytokines in response to poly I:C treatment. Additionally, AcMARCH5 exhibited an anti-apoptotic effect in H_2O_2-treated FHM cells. Collectively, these results suggest that AcMARCH5 may play a role in maintaining cellular homeostasis under disease and stress conditions in *A. clarkii*.

1. Introduction

The MARCH family represents a group of membrane-associated E3 ubiquitin ligases found in diverse organisms (Nagashima et al., 2014). This family consists of 11 members (MARCH 1 to 11), which share similar structures characterized by an N-terminal C4HC3-type RING domain and four transmembrane (TM) domains at the C-terminus (Nakamura et al., 2006; Zhang et al., 2019). The RING domain serves as the principal functional domain of MARCH, housing eight cysteine-histidine (Cys/His) residues that coordinate the zinc-binding sites. MARCH proteins harbor their TM domains in the outer mitochondrial membrane (OMM) and expose the RING-CH domain to the cytoplasm (Chu et al., 2021). Both E3 ligase activity and subcellular localization are essential for the proper function of MARCH genes (Gu et al., 2015).

MARCH5, a member of the MARCH family, plays a significant role in mitochondrial regulation and immune modulation in mammals (Karbowski et al., 2007; Rebl et al., 2011; Yoo et al., 2019). It regulates the activity of mitofusin-2 (Mfn2) and dynamin-related protein 1 (Drp1), controlling the fusion of the outer mitochondrial membrane (OMM) and the division of both the outer and inner mitochondrial membranes (Karbowski et al., 2007; Nakamura et al., 2006). In addition, MARCH5 is

* Corresponding author. Marine Molecular Genetics Lab, Department of Marine Life Sciences, Jeju National University, Jeju, 63243, Republic of Korea.
** Corresponding author. Department of Marine Life Sciences & Center for Genomic Selection in Korean Aquaculture, Jeju National University, Jeju 63243, Republic of Korea.
E-mail addresses: oneqiang@jejunu.ac.kr (Q. Wan), jehee@jejunu.ac.kr (J. Lee).

https://doi.org/10.1016/j.dci.2024.105283
Received 23 May 2024; Received in revised form 10 October 2024; Accepted 27 October 2024
Available online 29 October 2024

crucial for the degradation of MAVS aggregates during viral infections and for blocking retinoic acid inducible protein I (RIG-I)-like receptor (RLRs) signaling, thereby suppressing interferon and pro-inflammatory cytokine production (Yoo et al., 2015). This negative regulation of antiviral signaling by MARCH5 is critical for preventing excessive immune responses during viral infections (Yoo et al., 2015). Studies of hepatitis B virus (HBV)-associated liver disease have underscored the role of MARCH5 in the proteasomal degradation of hepatitis B viral x (HBx) protein aggregates, thus contributing to the mitigation of hepatic inflammation (Yoo et al., 2019). Moreover, MARCH5 participates in maintaining cell sensitivity to stress-induced apoptosis (Xu et al., 2016) and mitophagy (Lei et al., 2021). Inhibition of MARCH5 sensitizes cancer cells to anti-mitotic drugs by modulating the levels of the MCL1/NOXA protein complex in steady state and during mitotic arrest (Haschka et al., 2020).

MARCH5 has been identified in several teleost fish species. A duplication of MARCH5 gene (MARCH5A and MARCH5B) has been reported in rainbow trout (*Oncorhynchus mykiss*), suggesting that teleost possess an additional copy resulting from a fish-specific whole-genome duplication event. Furthermore, MARCH5A was found to be up-regulated in rainbow trout upon viral hemorrhagic septicemia virus (VHSV) infection (Rebl et al., 2011). Another study conducted in grass carp (*Ctenopharyngodon idellus*) showed elevated mRNA levels of MARCH5 following challenge with grass carp reovirus (GCRV), suggesting its involvement in the immune response (Ou et al., 2017). Nevertheless, the specific functional role of MARCH5 in the immune regulation of teleost remains unclear and requires further investigation.

The yellowtail clownfish (*Amphiprion clarkii*) is a member of the family Pomacentridae, naturally found in the coral reefs of the Indo-West Pacific. They play a significant role in the conservation of marine biodiversity and the resilience of marine ecosystems (Hirose, 1995). The popularity of *A. clarkii* in the tropical aquarium trade has increased due to their striking color morphs. To sustainably meet the rising market demand, it is essential to develop a responsible aquaculture system for this species (Kim et al., 2023). However, clownfish are vulnerable to diverse types of diseases, including bacterial, parasitic, fungal, and viral infections (Lam and Hue, 2021). Among bacterial diseases, vibriosis poses the greatest threat to clownfish, leading to symptoms such as tail rot, systemic infections, and even death (Marudhupandi et al., 2017). Viral infections, particularly lymphocystis caused by the lymphocystis disease virus (LCDV), are fatal and affect species like *Amphiprion ocellaris* and *Amphiprion clarkii* (Cheng et al., 2022). These findings highlight the importance of continued research on *A. clarkii* diseases to ensure the development of effective disease management strategies and to protect the species in both aquaculture and natural environments. This requires a comprehensive understanding of their innate immune system to formulate effective strategies against potential infectious diseases. Thus, present study aimed to address this knowledge gap by investigating the function of MARCH5 in *A. clarkii*. The study specifically investigated the molecular structure, tissue-specific distribution, temporal expression in response to immunostimulants, and its role in immune response and cellular stress. The findings of this study hold promise to enrich the current understanding of MARCH5 gene function in fish and contribute to the development of disease control strategies against various pathogens.

2. Materials and methods

2.1. In silico analysis of AcMARCH5

The coding sequence with the highest homology to the known AcMARCH5 gene sequence was identified from an *A. clarkii* transcriptome database constructed using Illumina® NovaSeq 6000 technology by Insilicogen, Korea (Shanaka et al., 2021). A putative open reading frame (ORF) was retrieved using the ORF finder tool (Marchler-bauer et al., 2017). The translated amino acid sequence was obtained from EMBOSS Transeq – EMBL-EBI (Madeira et al., 2022). Protein molecular weight and isoelectric point were calculated using the Expasy protparam online tool (https://web.expasy.org/compute_pi/). MARCH5 orthologs from other species were retrieved from the NCBI database using BLAST. Multiple sequence alignments were performed on selected orthologs in Clustal-Omega (Sievers and Higgins, 2017). Similarity and identity to other MARCH5 orthologs were analyzed by pairwise sequence alignment using the EMBOSS Needle (Rice et al., 2000). A phylogenetic tree was constructed using the neighbor-joining method with a bootstrap value of 5000 using MEGA11 software (Tamura et al., 2021). The protein domain structure of AcMARCH5 was annotated using the NCBI conserved domain search tool (Marchler-bauer et al., 2015) and DeepTMHMM tool (Hallgren et al., 2022). The two-dimensional visualization of AcMARCH5 was predicted using Domain Graph (DOG, version 1.0) software (Ren et al., 2009). The predicted AcMARCH5 three-dimensional tertiary structure was generated using the Iterative Threading ASSEmbly Refinement (I-TASSER) server (Zhang, 2008) and visualization and editing were performed using the PyMOL Molecular Graphic System (DeLano, 2002).

2.2. Experimental fish, immune challenge, and tissue collection

To perform the AcMARCH5 tissue specific expression analysis, five healthy *A. clarkii* fish with an average body weight of 20 g and body length of 10 cm were anesthetized with 40 mg/L of the tricaine mesylate (MS-222, Sigma-Aldrich, USA). Following anesthesia, the fish were individually dissected, and tissue samples were collected from the head kidney, spleen, liver, gill, intestine, kidney, brain, muscle, skin, heart, and stomach. Blood samples were collected using sterile, heparin sodium salt-coated syringes (Sigma, USA), and immediately centrifuged at 3000×*g* for 10 min at 4 °C to isolate the peripheral blood cells (PBCs). All tissue samples were immediately snap-frozen in liquid nitrogen and stored at −80 °C.

For the immune challenge experiment, acclimatized *A. clarkii* were randomly divided into four groups, each containing 25 individuals. Fish in each group were intraperitoneally injected with lipopolysaccharide (LPS) from *Escherichia coli* (0127:B8-Sigma) (2.5 μg/g), poly I:C (2.5 μg/g), or *Vibrio harveyi* (1×10^3 CFU/μL), suspended in 100 μL of sterile 1 × phosphate-buffered saline (PBS; pH 7.4). The control group was injected with 100 μL of sterile PBS. Tissue samples, including blood, spleen, and head kidney were collected from five individuals per group at 0, 6, 12, 24 and 48 h post injection (p.i.). All samples were immediately snap-frozen in liquid nitrogen and stored at −80 °C. For RNA extraction, biological replicates from each experimental group (at each time point), including those from the tissue-specific expression analysis ($n = 5$) and the immune challenge experiment ($n = 5$), were pooled separately. All experimental procedures performed in this study were reviewed and approved by the Animal Care and Use Committee of Jeju National University, Republic of Korea.

2.3. Total RNA extraction and cDNA synthesis

Total RNA was extracted from the isolated tissue samples using Trizol (Invitrogen, USA) and purified using RNeasy spin columns (Qiagen, Germany). Total RNA from cells was extracted using the RNeasy® Mini Kit (Qiagen, USA) according to the manufacturer's protocol. Agarose gel electrophoresis (1.5%) was performed to confirm the integrity of the purified RNA, and RNA concentration was measured using a μDrop plate (Thermo Scientific, USA). First-strand cDNA was synthesized using the PrimeScript™ II 1st strand cDNA Synthesis Kit (Takara, Japan) and stored at −80 °C after 40-fold dilution in nuclease-free water until required for subsequent experiments.

2.4. Transcriptional analysis of AcMARCH5 by real time quantitative polymerase chain reaction (RT-qPCR)

The tissue distribution and temporal expression level of *AcMARCH5* upon pathogenic stimulation were evaluated using RT-qPCR. Gene-specific qPCR primers were designed using the IDT PrimerQuest™ Tool (Owczarzy et al., 2008). The qPCR reaction mixture (10 μL) contained 3 μL of cDNA template, 5 μL of 2x TaKaRa Ex Taq TB Green® premix, 0.4 μL of each of forward and reverse primers (10 pmol/μL), and 1.2 μL of nuclease-free water. Thermal cycling conditions were as follows: denaturation at 95 °C for 10 s; 45 cycles of denaturing at 95 °C for 5 s, annealing at 58 °C for 10 s, extension at 72 °C for 20 s; and final extension at 95 °C for 15 s on a Thermal Cycler Dice™ TP950 (TaKaRa). Elongation factor 1 beta (*ef-1β*) from *A. clarkii* (MN970208) was used as the reference gene, and relative mRNA expression level was analyzed using the Livak $2^{-\Delta\Delta Ct}$ method (Livak and Schmittgen, 2001). Results are expressed as fold difference (mean ± standard deviation). The qPCR primers used in this study are listed in Supplementary Table 1.

To investigate AcMARCH5 functions, the coding DNA sequence (CDS) was cloned into the pcDNA3.1 (+) vector (Invitrogen, USA) using forward and reverse primers containing *Hind*III and *Xba*I restriction enzyme sites, respectively. Cloning and construction of expression plasmid. Additionally, the CDS was cloned into the pEGFP-N1 vector (Invitrogen, USA) using forward and reverse primers that contained *Hind*III and *Kpn*I restriction enzyme sites respectively, to access sub cellular localization. The primers used in the cloning experiments were listed in Supplementary Table 1. All recombinant plasmids were sequence confirmed, amplified in *E. coli* DH5α competent cells, and purified using the Qiagen® Plasmid Midi Kit.

2.5. Cell culture and plasmid DNA transfection

To analyze the functional roles and sub-cellular localization of AcMARCH5, fathead minnow (FHM) epithelial cells (ATCC, USA) were cultured in L-15 media (Sigma, St. Louis, MO, USA) supplemented with 10% (v/v) fetal bovine serum (FBS, Gibco-BRL; Life Technologies, Carlsbad, CA, USA) and 1% antibiotics (penicillin and streptomycin-Gibco-BRL; Life Technologies) at 25 °C. Murine macrophages (RAW 264.7) were cultured in Dulbecco's Modified Eagle's Medium (DMEM; Sigma, St. Louis, MO, USA) supplemented with 10% (v/v) FBS and 1% antibiotics. Cells were maintained in a humidified incubator at 37 °C and 5% CO_2.

Plasmid DNA transfection was performed using the X-tremeGENE™ 9 transfection reagent (Roche Diagnostics GmbH, Penzberg, Germany) according to the manufacturer's protocol. Briefly, 500 ng of the respective vector plasmids, 50 μL of Opti-MEM reduced serum-free medium (Thermofisher, USA), and 1.5 μL of X-tremeGENE™ 9 transfection reagent were mixed and incubated at 25 °C for 30 min. Subsequently, the transfection mixture was added to the well, and the cells were incubated for 24 h at appropriate temperatures until required for further treatments.

2.6. Subcellular localization assay

A subcellular localization assay was performed to predict the location of the protein within the cell. Briefly, FHM cells were transfected with 500 ng of empty pEGFP-N1 or pEGFP-N1- *AcMarch5* and further incubated for 24 h at 25 °C. After washing with 1 × PBS, 200 nM fluorescent probe Mito-Tracker™ Red (Invitrogen, USA) was added to the culture supernatant and incubated at 25 °C for 25 min. The cells were then washed with 1 × PBS and fixed with 1 mL of 4% formaldehyde in PBS for 15 min. The cells were washed again with 1 × PBS, stained with NucBlue™ Fixed Cell Ready Probes™ Reagent (DAPI - 4′,6-diamidino-2-phenylindole) (Invitrogen, USA), and incubated for 20 min at 25 °C. A fluorescence microscope (Leica DM6000 B; Leica Microsystems, Wetzlar, Germany) was used to image the cells at 400 × magnification. Cell images were further analyzed using Leica Application Suite X Software (Version 3.3).

2.7. Evaluation of antiviral potential of AcMARCH5 against VHSV

To assess the impact of AcMARCH5 under viral stimulation, FHM cells were seeded in a 12-well plate at a density of 2.5×10^5 cells/well and transfected with 500 ng of pcDNA3.1(+) or pcDNA3.1(+)-*AcMarch5* at 25 °C for 24 h. Cells were infected at 0.01 multiplicity of infection (MOI) of VHSV virus (FWando05 strain isolated from diseased olive flounder in Korea) in L-15 medium supplemented with 5% FBS and 0.5% of antibiotics (penicillin and streptomycin) and incubated at 20 °C. Cells were harvested at 0, 12, and 24 h post-infection (h p.i.) and total RNA was extracted using the RNeasy® Mini Kit (Qiagen, USA). The mRNA expression levels of VHSV encoded proteins as well as mitochondrial antiviral-signaling (*mavs*), TANK-binding kinase 1 (*tbk1*), interferon type I (*ifn-I*), interferon regulatory factor 7 (*irf7*), and interferon regulatory factor 3 (*irf3*) were analyzed using RT-qPCR using gene specific primers as detailed in Supplementary Table 1. In addition, the viral copy numbers were determined from the absolute expression of VHSV-N protein using the VHSV standard curve (Kim et al., 2014). Further validation of VHSV replication in FHM cells was performed using fluorescence images captured following the infection of rVHSV-ΔNV-EGFP, donated by the Professor Kihong Kim at Pukyong National University, Republic of Korea (Wijerathna et al., 2022).

2.8. Analysis of cytokine expression upon poly I:C treatment

Murine macrophages (RAW 264.7) cells were seeded in a 96-well plate at a density of 1×10^5 cells/well. After incubation at 37 °C the cells were transfected with pcDNA3.1(+) empty vector or pcDNA3.1 (+)-*AcMarch5*. After 24 h of incubation at 37 °C, each well was treated with 100 μL of 20 μg/mL Poly I:C and incubated at 37 °C. To evaluate the mRNA expression of the cytokines, including interleukin 6 (*il-6*), interleukin 1 beta (*il-1β*), and tumor necrosis factor alpha (*tnf-α*), the AcMARCH5-overexpressed and control RAW 264.7 cells were harvested at 0, 12, and 24 h and subjected to RT-qPCR as described previously.

2.9. Analysis of cell apoptosis by propidium iodide (PI)/Hoechst 33342 dual staining and expression analysis of apoptotic genes

The PI/Hoechst 33342 double staining assay was performed in FHM cells to analyze the effect of AcMARCH5 on H_2O_2-induced cell apoptosis. FHM cells were seeded in 12-well plates at a density of 3×10^5 cells/well, followed by transfection with pcDNA3.1(+) or pcDNA3.1 (+)-*AcMarch5*. After incubation for 24 h at 25 °C, the cells were treated with H_2O_2 at a final concentration of 2 mM. The cells were then stained with 5 μg/mL of PI and 20 μg/mL of nuclear-specific blue-fluorescent Hoechst 33342 dye (Sigma-Aldrich) to visualize the compacted state of chromatin in apoptotic cells. Dual staining patterns were captured using a fluorescence microscope at 400 × magnification (Leica DM6000 B; Leica Microsystems, Wetzlar, Germany). Additionally, a distinct staining procedure was performed with Hoechst 33342 dye to quantify the apoptotic body index after the observations of nuclear chromatin condensation in each treatment group. The following equation was used to evaluate the apoptotic body index: Apoptotic body index = $(n[T_b/N_t]/n[C_b/N_c])$, where N_t indicates the total number of nuclei in each treatment separately, N_c indicates the total number of nuclei in untreated pcDNA3.1(+)-transfected cells, T_b and C_b indicate the number of apoptotic bodies in H_2O_2-treated and untreated cells respectively while n indicates the mean values (Wijerathna et al., 2022).

To analyze the activation of apoptotic signaling, cells in each treatment group were harvested separately at 24 h, followed by RNA isolation and cDNA synthesis to analyze the transcript levels of Bcl-2-associated X (*Bax*), and B-cell lymphoma 2 (*Bcl-2*) using RT-qPCR. The primers used for RT-qPCR analysis are listed in Supplementary Table 1.

A separate experiment was conducted to assess caspase levels following H_2O_2-induced apoptosis in FHM cells. Initially, FHM cells were seeded in a 12-well plate at a density of 3×10^5 cells per well. Upon reaching 80% confluency, the cells were transfected with either the pcDNA3.1(+) empty vector or pcDNA3.1(+)-*AcMarch5*. After 24 h of incubation at 25 °C, caspase levels were measured using the Caspase-Glo® 3/7 Assay Kit, following the manufacturer's protocol.

2.10. Statistical analysis

All experiments were performed in triplicate, and the results were expressed as mean ± standard deviation. One-way analysis of variance (ANOVA) was used for the statistical analysis of tissue specific distribution results. Data from immune challenge experiments and other functional assays were analyzed using the Student's *t*-test. p-value <0.05 was used to indicate the significance.

3. Results

3.1. In silico analysis of AcMARCH5

The cDNA sequence of AcMARCH5 was obtained from the *A. clarkii* transcriptome database previously constructed in the laboratory and subsequently submitted to the NCBI database under the accession number OR670423. The putative open reading frame (ORF) of AcMARCH5 was 864 bp in length, encoding 287 amino acids. The molecular weight and theoretical isoelectric point of AcMARCH5 protein were predicted to be 32.02 kDa and 9.11 pI, respectively. Structural analysis revealed that AcMARCH5 consisted of an N-terminal RING-CH domain and four C-terminal transmembrane domains (Fig. 1A). The 3D protein structure of AcMARCH5 predicted using I-TASSER achieved a confidence score (C-score) of −4.57 (Fig. 1B).

Multiple sequence analysis revealed the conservation of amino acids of AcMARCH5 with other vertebrate orthologs (Fig. 2). Notably, the domains in the N-terminal region showed greater conservation than those in the C-terminal region. Supplementary Table 2 illustrates the pairwise identity and similarity of AcMARCH5 with other vertebrate orthologs. AcMARCH5 displayed the highest identity (94.4%) and similarity (95.8%) to MARCH5 from *Amphiprion ocellaris*, a species within the same genus. Furthermore, the phylogenetic tree showed that AcMARCH5 was clustered together with MARCH5 orthologs in the fish clade, with high bootstrap values (Fig. 3).

3.2. Subcellular localization of AcMARCH5 in FHM cells

The subcellular localization of the AcMARCH5 protein was examined by fluorescence imaging analysis of FHM cells following transfection with either the pEGFP-N1 plasmid or the pEGFP-N1-*AcMarch5* construct (Fig. 4). In contrast to the uniform distribution of GFP observed in pEGFP-N1 plasmid-transfected cells, cells expressing GFP-tagged AcMARCH5 exhibited concentrated green spots dispersed around the DAPI-stained nucleus (appearing blue). Furthermore, the green fluorescence signal of AcMARCH5 perfectly co-localized with the red fluorescence signal of MitoTracker™, resulting in a yellow hue in the merged image. These findings revealed that the AcMARCH5 protein predominantly localizes to the mitochondria.

3.3. Tissue distribution of AcMARCH5 mRNA

Analysis the *AcMARCH5* mRNA expression profile in 12 different *A. clarkii* tissues (head kidney, spleen, liver, gill, intestine, kidney, brain, muscle, skin, heart, stomach, and blood) using RT-qPCR unveiled ubiquitous expression in all tested tissues (Fig. 5). The highest level of *AcMARCH5* mRNA expression was observed in the muscle (5.43 ± 0.55 fold), followed by moderate expression in the brain (3.78 ± 0.11 fold), kidney (3.19 ± 0.32 fold), and gill (2.31 ± 0.17 fold). Expression levels

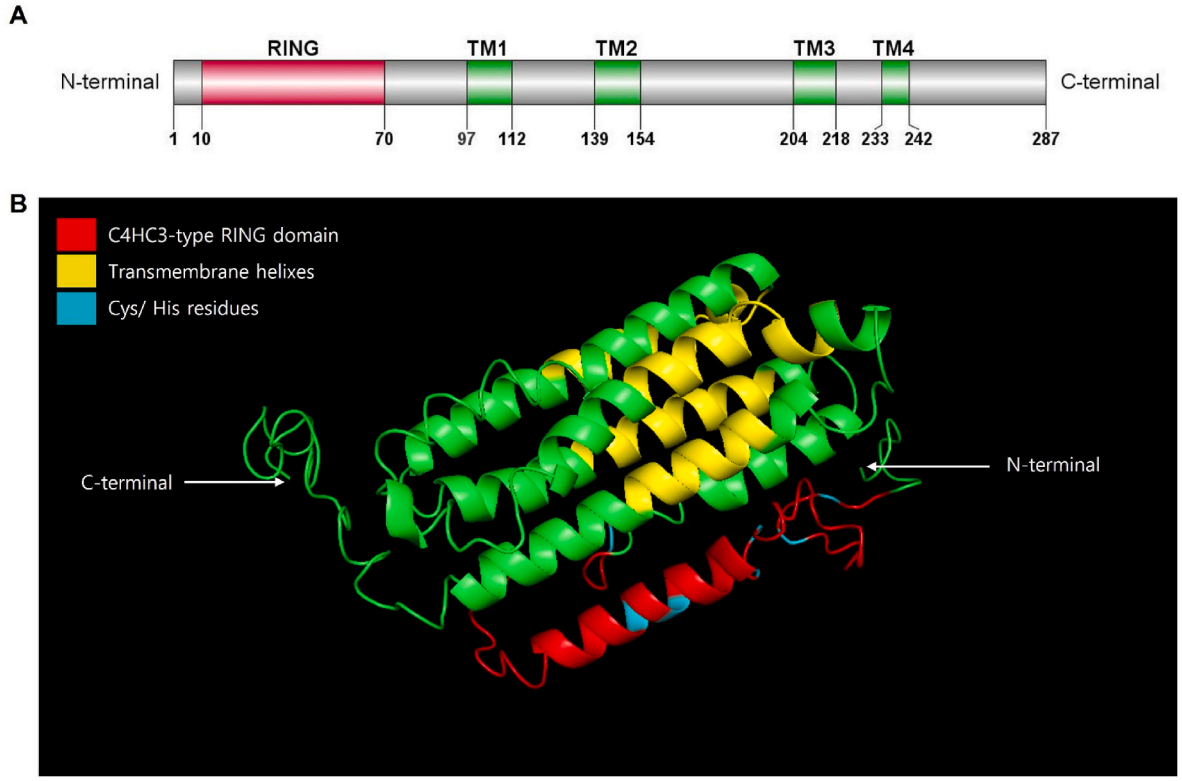

Fig. 1. Schematic illustration of domains structure (A) and predicted 3D structure of AcMARCH5 (B). Protein domain structure of AcMARCH5 was annotated using NCBI conserved domain search tool and DeepTMHMM tool. (RING: RING-CH domain; TM1,TM2, TM3, TM4: Transmembrane domain 1, 2, 3, and 4 respectively). The 3D structure was predicted using I-TASSER server and visualized using the PyMOL software.

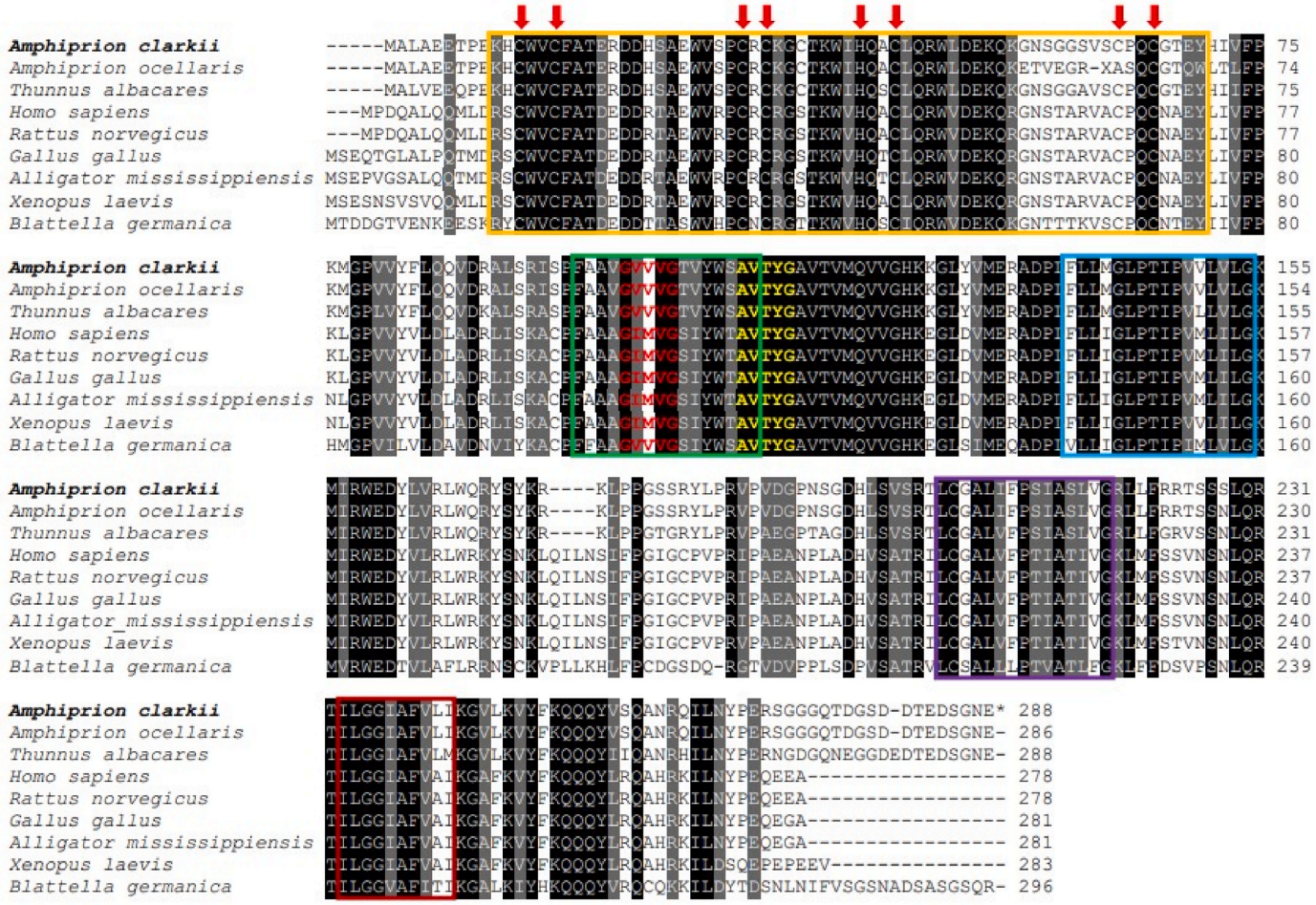

Fig. 2. Multiple sequence alignment of AcMARCH5 with vertebrate orthologs. Fully conserved and partially conserved amino acids are shaded in black and gray respectively. RING-CH domain, transmembrane domain 1,2,3, and 4 are indicated by yellow, green, blue, purple, and red squares respectively. Furthermore, Red color down arrows indicate the Cys/His residues of the C4HC3 motif inside the RING domain. The GxxxG and AxxxG motifs have been indicated in red and yellow bolded letters respectively. (For interpretation of the references to color in this figure legend, the reader is referred to the Web version of this article.)

in all other tissues were relatively low.

3.4. Temporal analysis of AcMARCH5 mRNA expression upon immune stimulation

The temporal mRNA expression of *AcMARCH5* in the blood, spleen, and head kidney of *A. clarkii* after stimulation with Poly I:C, LPS, or *V. harveyi* showed a consistent pattern (Fig. 6). The expression was gradually upregulated at early time points (6–24 h) and subsequently downregulated at later time points (48–72 h). Among the three stimuli, Poly I:C exerted the strongest modulatory effect on the *AcMARCH5* mRNA expression level, with peak expression at 24, 6, and 12 h in blood, spleen, and head kidney, respectively. In contrast, LPS and *V. harveyi* treatments showed a comparatively lower induction of *AcMARCH5* mRNA expression in blood and spleen tissues, with the highest expression observed at 6 h for both treatments.

3.5. AcMARCH5 positively regulates VHSV replication in FHM cells

To investigate the role of AcMARCH5 in viral infection, VHSV replication was examined in AcMARCH5-overexpressed FHM cells at both 12 and 24 h post-infection (p.i.) (Fig. 7A–F). Overexpression of AcMARCH5 significantly increased the expression of six viral genes and the VHSV copy numbers at 12 and 24 h p.i. compared to the control cells (Fig. 7G). In addition, pcDNA3.1(+)-*AcMarch5* transfected FHM cells showed higher GFP fluorescence of recombinant VHSV than the control cells at 24 h p.i., indicating an enhancement on viral replication (Fig. 7H).

3.6. AcMARCH5 attenuates the RLR signaling pathway and negatively regulates the antiviral gene expression during viral infection

To understand the mechanism underlying AcMARCH5-enhanced viral replication, the mRNA expression of *mavs*, *tbk1*, *ifn-I, irf7, and irf3* was examined in VHSV-infected FHM cells (Fig. 8). Notably, distinct expression patterns of these genes were observed in the AcMARCH5-overexpressed FHM cells compared to control cells. In AcMARCH5-overexpressed FHM cells, the mRNA expression levels of *mavs* and *tbk1* were significantly lower than those in pcDNA3.1(+)-transfected control cells at both 12 and 24 h p.i. (Fig. 8A and B), indicating decreased activation of the RLR signaling pathway. Furthermore, the expression levels of three genes (*ifn-I, irf7, and irf3*) also showed a significant reduction in AcMARCH5-overexpressed cells compared to control cells at both 12 and 24 h p.i. (Fig. 8C–E), indicating a negative regulatory effect on the antiviral gene activation.

3.7. AcMARCH5 attenuates pro-inflammatory cytokines production in macrophages following poly I:C stimulation

To investigate the effect of AcMARCH5 on pro-inflammatory cytokine production, the mRNA expression levels of *il-6*, *il-1β*, and *tnf-α* were assessed in RAW 264.7 cells at different time points after Poly I:C

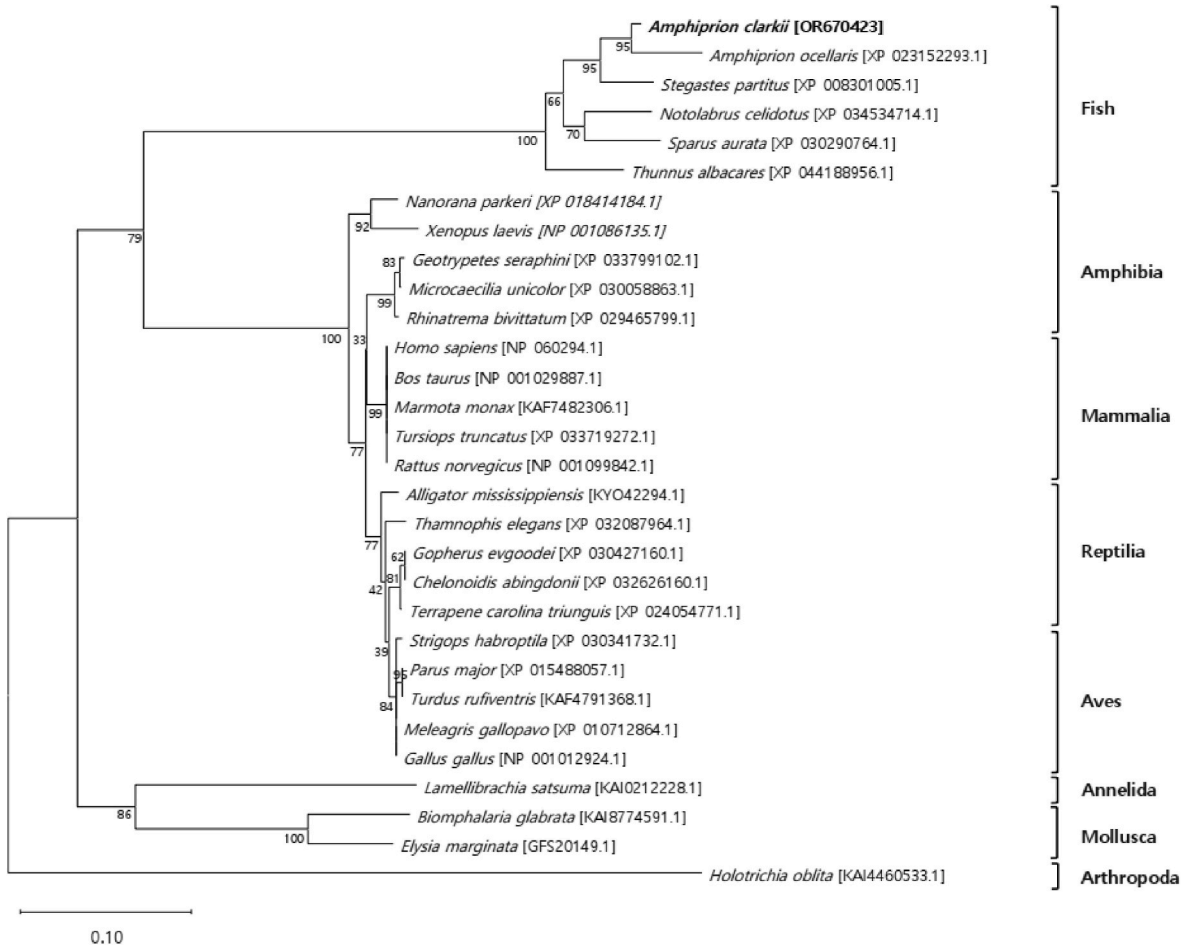

Fig. 3. Phylogenetic relationship of AcMARCH5 with other vertebrate orthologs. The phylogenetic tree was constructed using the neighbor-joining method with MEGA software. Numbers at each node represent the bootstrap confidence values after 5000 replications. NCBI accession numbers were mentioned next to the scientific name.

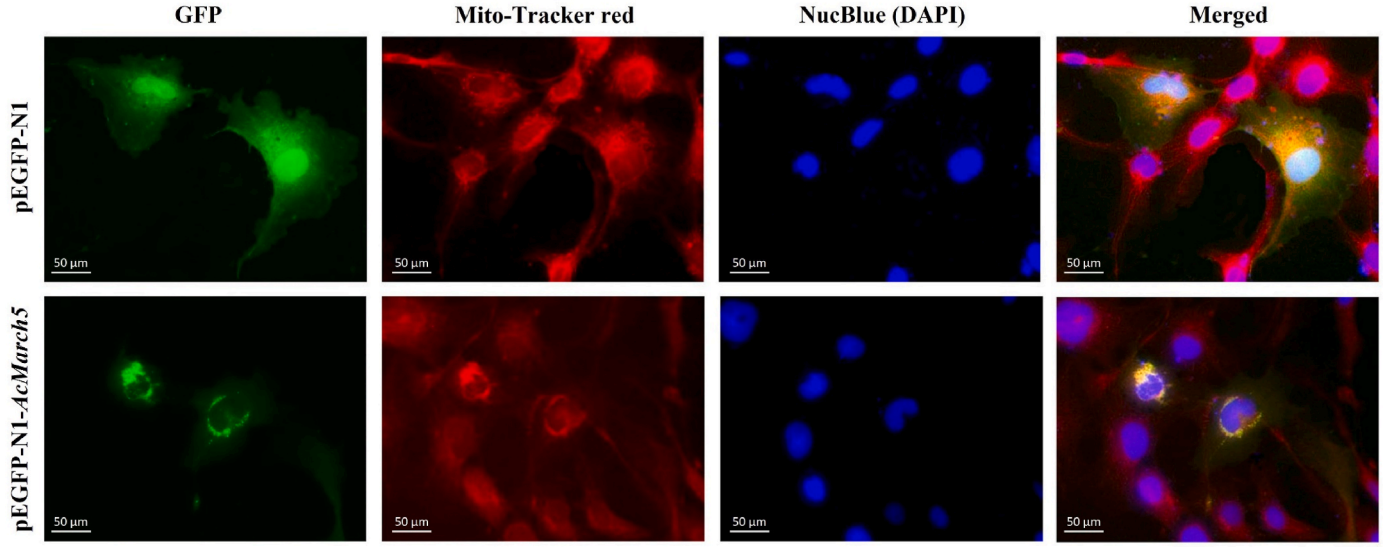

Fig. 4. Fluorescence images of subcellular localization of AcMARCH5 in FHM cells. Cells were transiently transfected with pEGFP-N1 or pEGFP-N1-*AcMarch5*. After incubation at 25 °C for 24 h, Mito-Tracker was added to the culture supernatant. Cells were then fixed with 4% formaldehyde and stained with DAPI to visualize the nucleus. A fluorescence microscope was used for capturing the images. Green, red, and blue colors showed the expression of pEGFP-N1 or pEGFP-N1-*AcMarch5*, stained mitochondria, and nucleus in the images respectively. Merged image indicated the fluorescence expression of pEGFP-N1 or pEGFP-N1-*AcMarch5*, mitochondria, and nucleus together in the same cell. (For interpretation of the references to color in this figure legend, the reader is referred to the Web version of this article.)

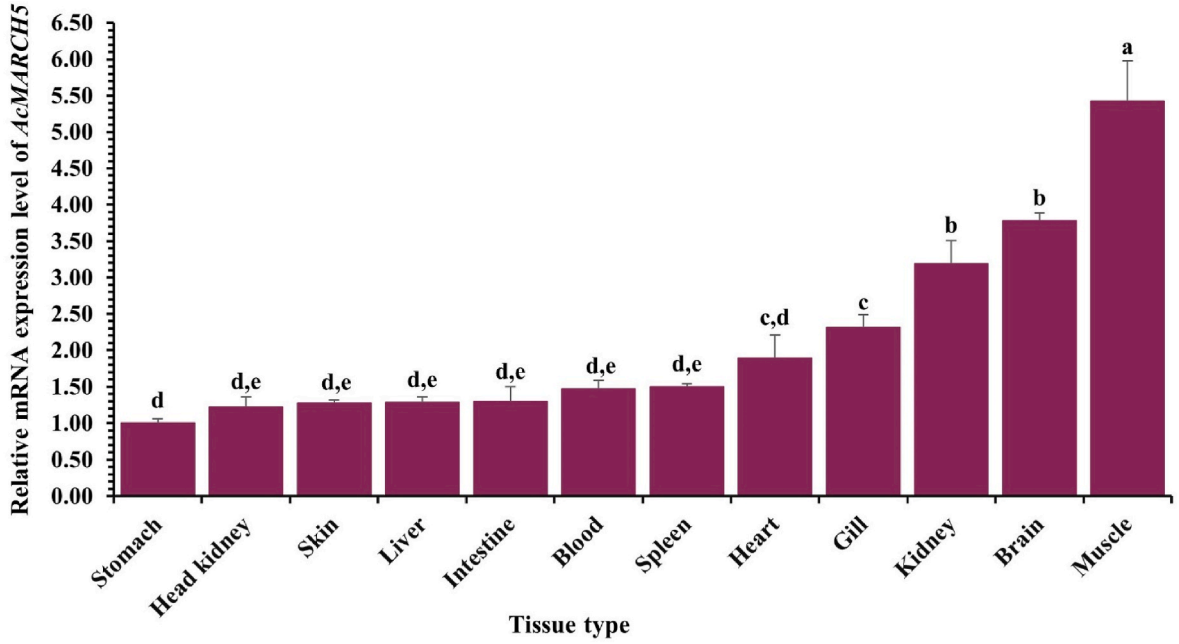

Fig. 5. Tissue-specific relative mRNA expression profile of *AcMARCH5* in different tissues of *A. clarkii* under normal physiological condition. Data were presented relative to the mRNA expression level in the stomach (the tissue with the lowest expression level). Statistical significance was performed using the one-way analysis of variance (ANOVA) with Tukey's test. Data were presented as the mean values of relative mRNA expression level ± standard deviation (SD) ($n = 3$). Different letters indicate the statistical difference between each type of tissues ($p < 0.05$).

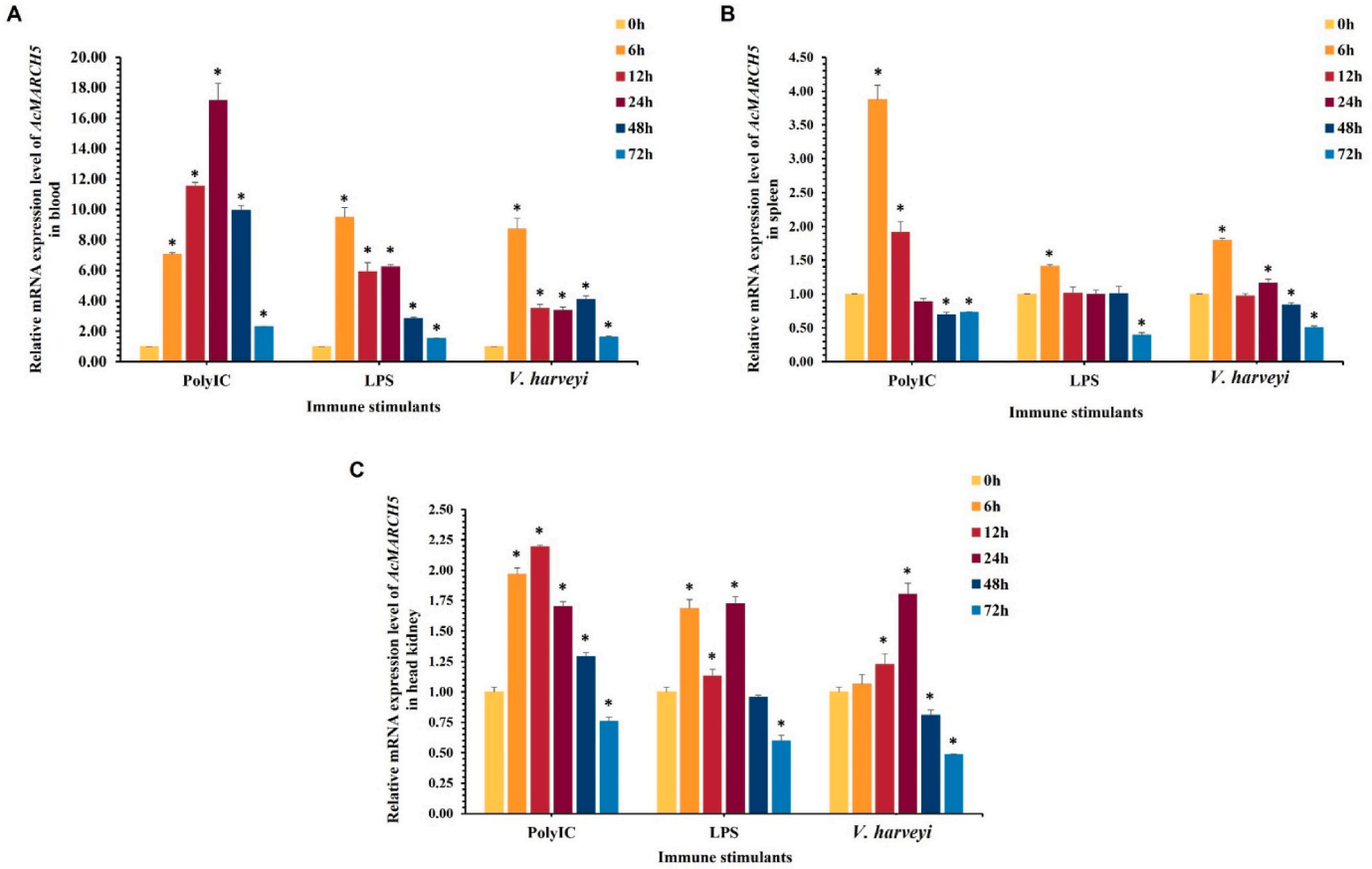

Fig. 6. Relative mRNA expression level of *AcMARCH5* in the blood (A), spleen (B), and head kidney (C) of *A. clarkii* after immune stimulation. Transcription levels of *AcMARCH5* were detected using RT-qPCR analysis after stimulation with Poly I:C, LPS or *Vibrio harveyi* at the time points of 0, 6, 12, 24, 48, and 72 h. Data were presented as the mean values of relative mRNA expression level ± standard deviation (SD) ($n = 3$). Untreated control at 0 h was used as the basal value to normalize the fold expression values of experimental groups. *Statistical significance of each group was calculated using the Student's *t*-test ($p < 0.05$).

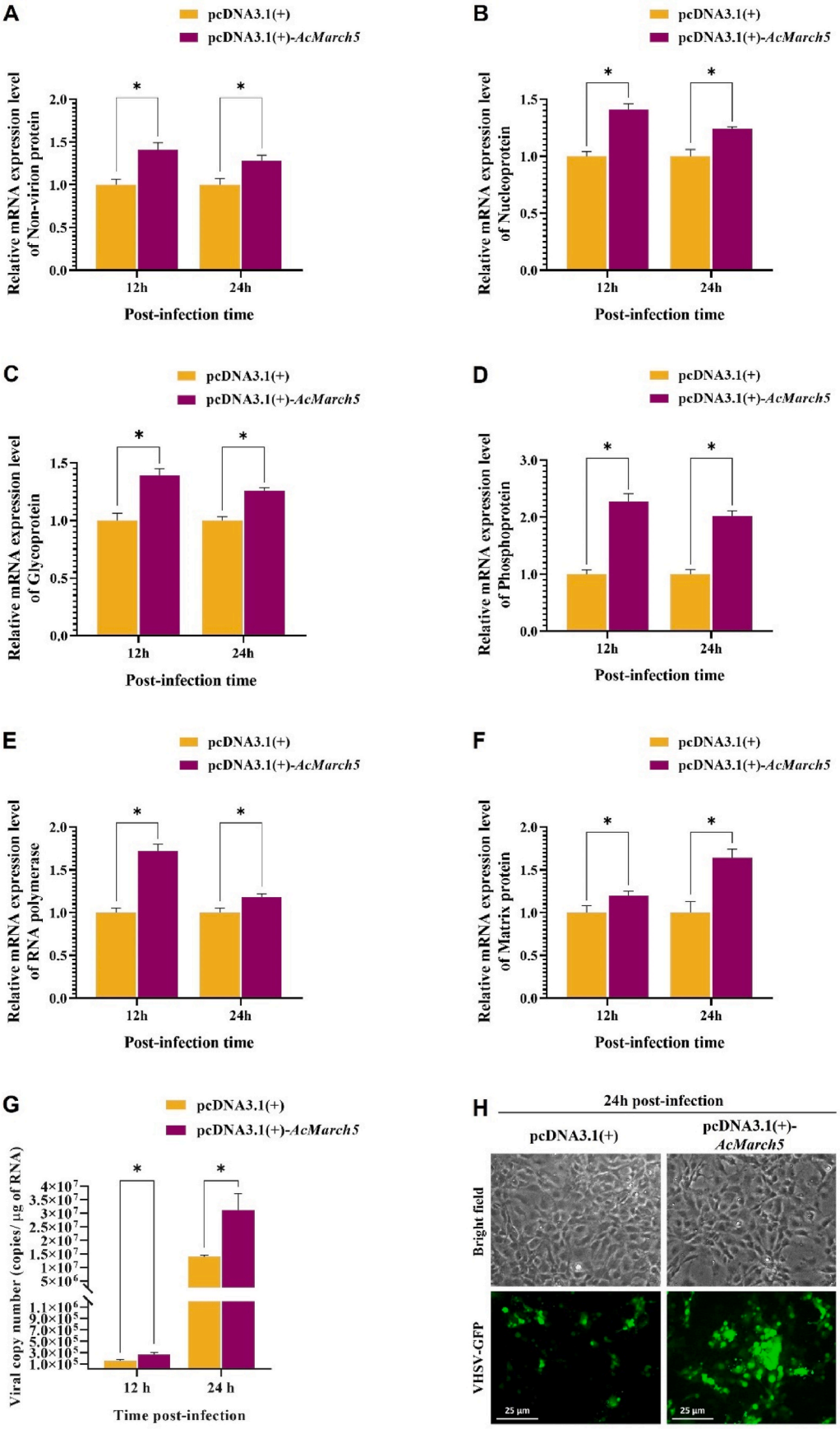

(caption on next page)

Fig. 7. *In vitro* analysis of VHSV replication in FHM cells. FHM cells were transfected with pcDNA3.1(+) or pcDNA3.1(+)-*AcMarch5* separately. After incubation of 24 h, VHSV infection was done (0.01 MOI). Relative mRNA expression levels of VHSV encoded Non-virion protein (A), Nucleoprotein (B), Glycoprotein (C), Phosphoprotein (D), RNA polymerase (E), and Matrix protein (F) were analzyed by qRT-PCR.VHSV copy number per 1 μg of RNA was calculated by a standard curve based on Nucleoprotein expression level (G). Simultaneous white light and fluorescence images of FHM cells infected with rVHSV-ΔNV-EGFP (green color) at 24 h p. i. (H). Data were expressed as mean ± SD ($n = 3$). Statistical significance ($p < 0.05$) of each group was determined using the Student's *t*-test and indicated with an asterisk (*). (For interpretation of the references to color in this figure legend, the reader is referred to the Web version of this article.)

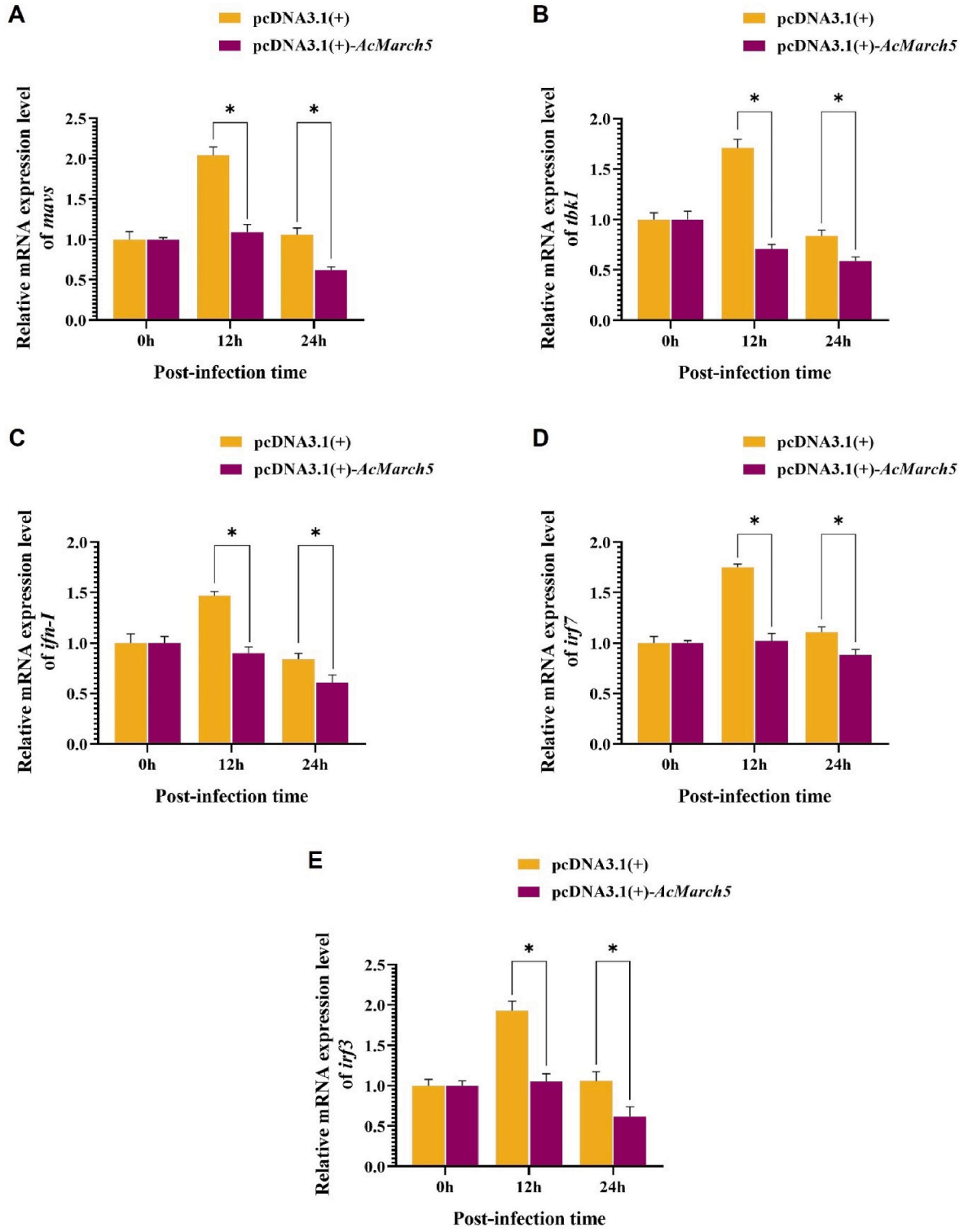

Fig. 8. Relative mRNA expression levels of genes in RLR signaling pathway. The expression of *mavs* (A), *tbk1* (B), *ifn-I* (C), *irf7* (D), and *irf3* (E) was evaluated by RT-qPCR in pcDNA3.1(+) vector and pcDNA3.1(+)-*AcMarch5*-transfected FHM cells followed by VHSV infection. Data were expressed as mean ± SD ($n = 3$). Statistical significance ($p < 0.05$) of each group was determined using the Student's *t*-test and indicated with an asterisk (*).

treatment (Fig. 9). Both AcMARCH5-overexpressed and control cells showed notable increase in the expression of all three pro-inflammatory cytokine genes after Poly I:C treatment. However, overexpression of AcMARCH5 significantly attenuated the induction of pro-inflammatory cytokine gene expression by Poly (I:C).

3.8. *AcMARCH5 diminishes apoptosis, Bax/Bcl-2 ratio increment, and caspase activity during H_2O_2-induced oxidative stress*

To investigate the role of AcMARCH5 in apoptosis regulation, the fluorescence images of the PI/Hoechst dual staining patterns in FHM cells transfected with pcDNA3.1(+) or pcDNA3.1(+)-*AcMarch5* followed by H_2O_2 exposure were displayed (Fig. 10A). After 24 h of H_2O_2 exposure, AcMARCH5-overexpressed cells showed significantly higher levels of cell viability than pcDNA3.1(+)-transfected cells. Moreover, the apoptotic body index significantly reduced in AcMARCH5-overexpressed FHM cells subjected to H_2O_2 exposure (Fig. 10B). The images used for apoptotic body quantification are provided in Supplementary Fig. 1. In AcMARCH5-overexpressing FHM cells, the *Bax/Bcl-2* ratio showed a significantly diminished increase compared to cells transfected with pcDNA3.1(+) (Fig. 10C). Additionally, the relative activity of caspase-3/7 was significantly reduced in the AcMARCH5-overexpressing cells (Fig. 10D).

4. Discussion

Mammalian MARCH5 plays an essential role in ubiquitination, which is critical for immune regulation and several fundamental cellular processes, such as cell differentiation, DNA repair, and apoptosis (Zheng and Tang, 2021). Nevertheless, the precise function of teleost MARCH5, particularly in the context of its involvement in the immune response against pathogenic infections, remains inadequately elucidated. Hence, this study sought to assess the molecular characteristics of MARCH5 in *A. clarkii*, along with *in vivo* and *in vitro* immunoregulatory functions.

All 11 members of the MARCH family, with the exception of MARCH7 and MARCH10, exhibit relatively conserved structural properties (Zheng and Tang, 2021). Structural analysis of AcMARCH5 revealed the presence of characteristic RING-CH domain. Similar to other members of the MARCH family (Chu et al., 2021), the overall structure of the RING domain in AcMARCH5 is maintained by conserved cysteine and histidine residues that exist in the core of the domain, along with two coordinating zinc atoms (Deshaies and Joazeiro, 2009). Multiple sequence alignment of AcMARCH5 with orthologs in other vertebrates unveiled a highly conserved region at the N-terminus rather than the C-terminus. Furthermore, AcMARCH5 displays two GxxxG motif variants: a partially conserved GxxxA in the central part of the TM1 domain and a highly conserved AxxxG in the tail part of the TM1 domain. These two motifs are known to mediate oligomerization, intramolecular helix–helix interactions, and protein–protein

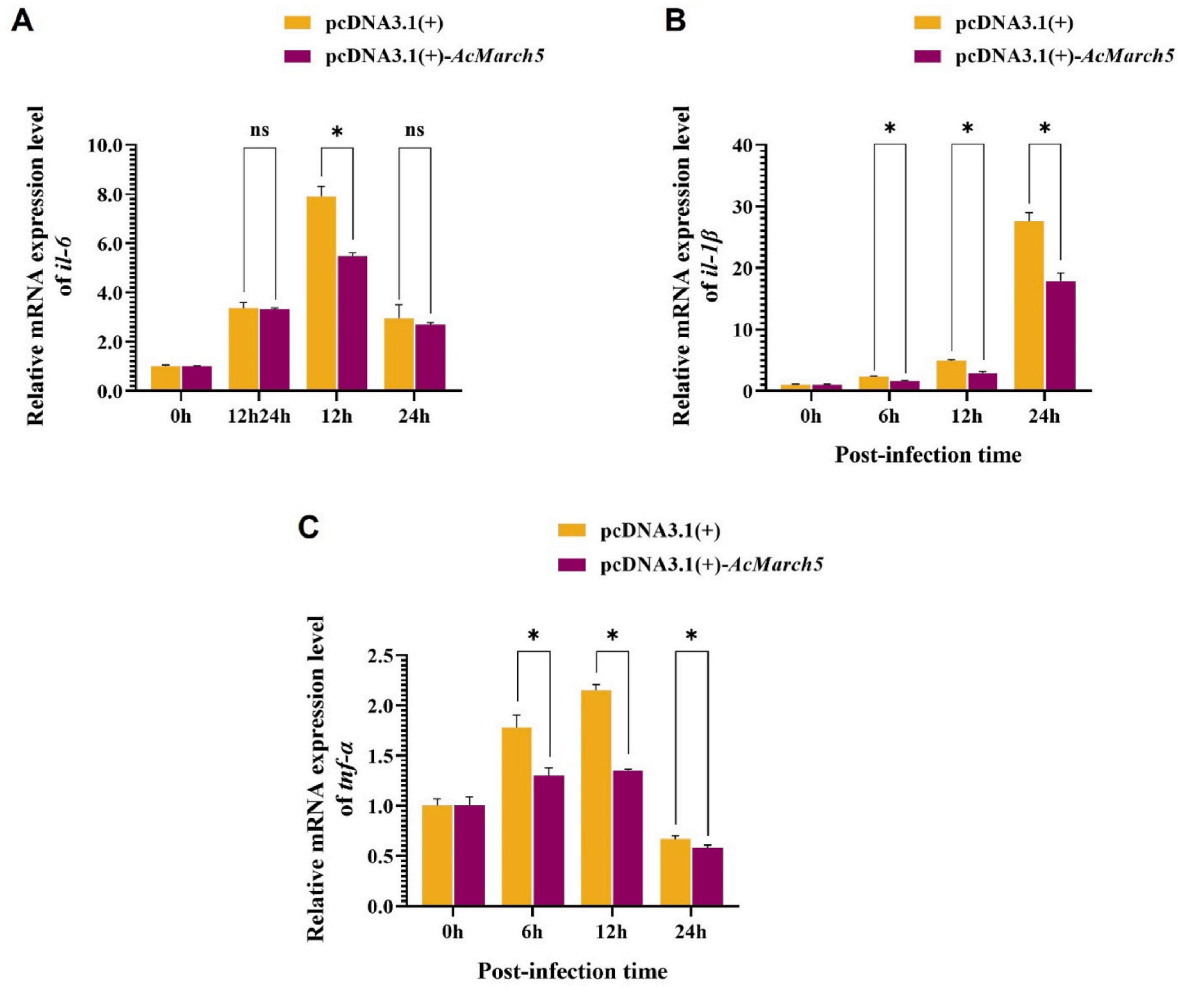

Fig. 9. Relative mRNA expression levels of inflammatory cytokines in RAW 264.7 murine macrophage cells after stimulation with Poly I:C. RAW 264.7 macrophage cells were transfected with pcDNA3.1(+) vector and pcDNA3.1(+)-*AcMarch5*. The expression of *il-6*, *il-1β* and *tnf-α* (A–C) was analyzed by qRT-PCR. Data were represented as mean ± SD ($n = 3$). Statistical significance ($p < 0.05$) of each group was determined using the Student's *t*-test and indicated with an asterisk (*).

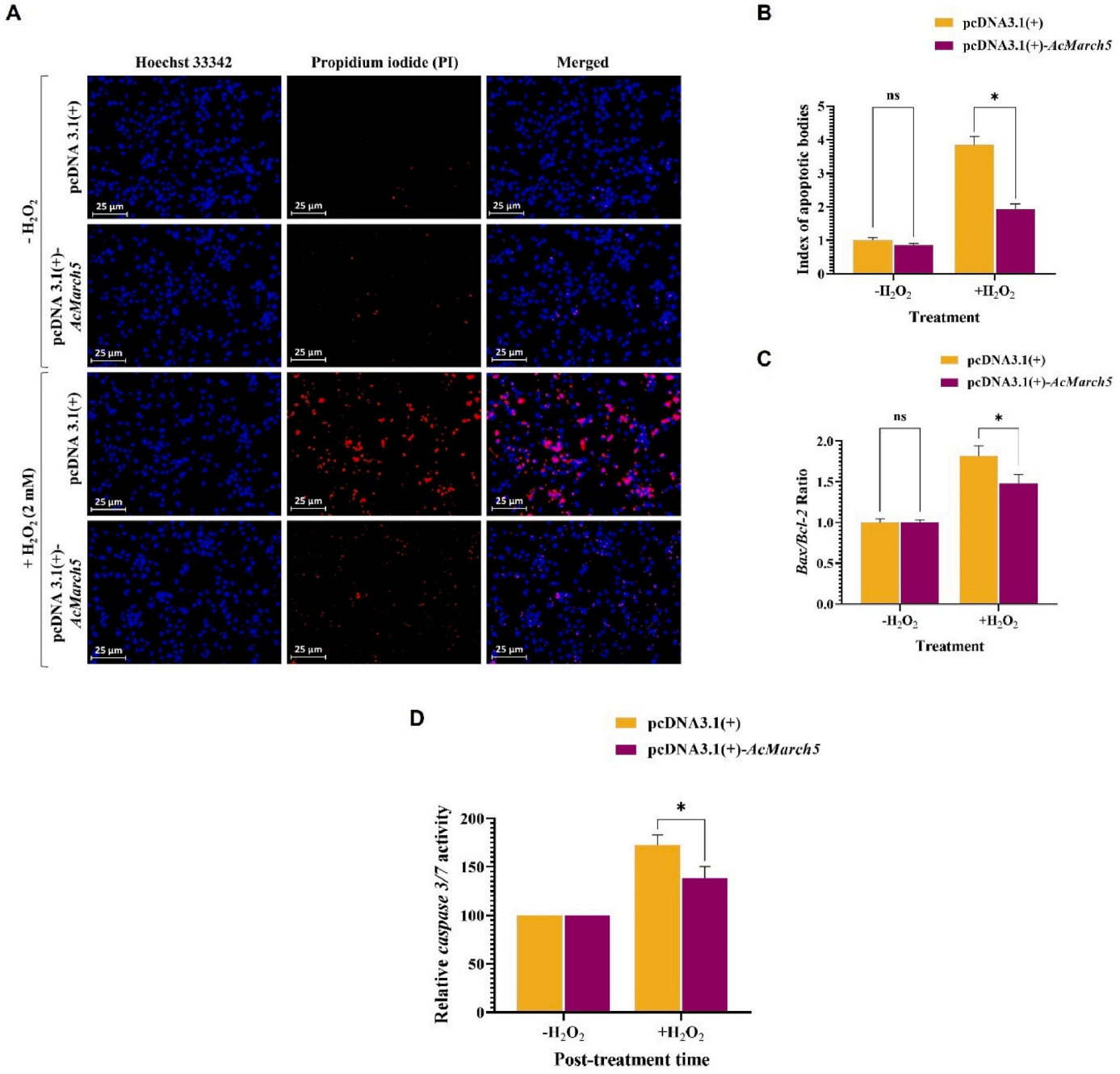

Fig. 10. Anti-apoptotic effect of AcMARCH5 in H_2O_2 induced oxidative stress. FHM cells were transfected with pcDNA3.1(+) or pcDNA3.1(+)-*AcMarch5* separately and exposed to 2 mM of H_2O_2. PI/Hoechst dual staining assay was performed after 24 h of incubation at 25 °C to visualize the viable cells (A). Apoptotic body index in FHM cells exposed to 2 mM of H_2O_2 at 24 h (B). Apoptotic body index was represented as the number of apoptotic bodies relative to the total number of cells in each treatment separately. Ratio of *Bax/Bcl-2* expression (C), relative activity of *caspase-3/7* (D) were assessed after 24 h of 2 mM H_2O_2 treatment. The Data were presented as a mean index of apoptotic bodies ± SD ($n = 3$). Statistical significance ($p < 0.05$) of each group was determined using the Student's *t*-test and indicated with an asterisk (*).

interactions (Bauer et al., 2017). Mutation of the GxxxG motif to LxxxL has been shown to impede MARCH5 oligomerization (Kim et al., 2016). Pairwise sequence alignments of MARCH5 orthologs from different species across diverse taxonomies showed identities greater than 50%, indicating structural and functional conservation of MARCH5 genes throughout evolution.

Members of the MARCH family exhibit diverse cellular localization patterns, with each protein's function directly impacted by its subcellular localization (Lin et al., 2019). For instance, MARCH1, 2, 3, 8, and 9 are predominantly localized in endosomes, lysosomes, and the plasma membrane (Bartee et al., 2004; Fukuda et al., 2006; Goto et al., 2003; Jabbour et al., 2009; Nakamura et al., 2005; Rigotti et al., 2017), whereas MARCH4, MARCH6, MARCH10, and MARCH11 are located in the Golgi apparatus, endoplasmic reticulum (ER), cytosol, and multi-vesicular bodies (MVBs), respectively (Bartee et al., 2004; Hassink et al., 2005; Iyengar et al., 2011; Morokuma et al., 2007). Fluorescence imaging revealed the subcellular localization of AcMARCH5 in the mitochondria of FHM cells. Ample evidence supports the assertion that the MARCH5 protein localizes to the outer membrane of mitochondria in mammalian cells (Nakamura et al., 2006; Yonashiro et al., 2006). This

localization of the MARCH5 protein to the mitochondria is believed to play a critical role in the regulating RLR family receptors (Lin et al., 2019).

Tissue distribution analysis revealed relatively high levels of *AcMARCH5* expression in muscle and brain tissues. Skeletal muscle and brain are tissues characterized by high energy demands and substantial mitochondrial abundance, rendering them more susceptible to mitochondrial diseases. Hence, the regulation of mitochondrial health is pivotal in these tissues (Bond et al., 2018; Frost and Lang, 2008; Qin and Xi, 2022). Several other MARCH proteins, such as MARCH2 and MARCH9, exhibit higher abundance in a panel of human tissue samples. However MARCH4 displays limited expression across tissues, with higher expression in brain and placenta (Bartee et al., 2004). The heightened expression of *AcMARCH5* mRNA in muscle and brain tissues suggests its potential role in modulating mitochondrial quality, governing associated proteins, and thereby contributing to mitochondrial homeostasis and cell survival in *A. clarkii* (Park et al., 2014).

The immune response of *AcMARCH5* expression was investigated in the blood, spleen, and head kidney, given the significance of these three tissues in the fish immune system (Dahle et al., 2015; Jiang et al., 2020; Passantino et al., 2002). Poly I:C served as a potent immunostimulant capable of activating the RLR signaling pathway (Fortier et al., 2023). In mammalian cells, MARCH5 targets MAVS aggregates and efficiently degrades them via the ubiquitin-proteasome pathway, thereby terminating MAVS signaling (Yoo et al., 2015). Additionally, MARCH5 is responsible for binding to activated RIG-I and mediating with proteasome-dependent degradation to shut down RLR signaling (Park et al., 2020). This may explain the significant increase in *AcMARCH5* in response to Poly I:C treatment in *A. clarkii*. Furthermore, Yoo et al. reported that following the initial transcriptional activation triggered by viral dsRNA mimics, murine MARCH5 undergoes auto-ubiquitination (Yoo et al., 2015), leading to a reduction in its protein level (Yonashiro et al., 2006). This finding aligns with our observation of a gradual reduction in *AcMARCH5* expression after 24 h p.i. *V. harveyi* is a Gram-negative bacterial pathogen known to impact marine fish aquaculture (Zhang et al., 2020), while LPS serves as a key component of the cell wall of Gram-negative bacteria. Upon encountering these challenges, the immune response is likely initiated via activation of Toll-like receptor 4 (TLR4) (Lu et al., 2008), along with downstream signaling molecules including TRAF6 (Akira, 2003). Previous research has demonstrated that MARCH5 catalyzes the polyubiquitination of TANK, thereby suppressing its inhibitory action on TRAF6 (Shi et al., 2011), which aids in activating downstream signaling pathways to counteract pathogenic invasion. The observed upregulated mRNA expression of *AcMARCH5* upon challenges with *V. harveyi* and LPS may potentially contribute to the immune regulation in response to bacterial infections.

During VHSV infection in FHM cells, AcMARCH5 overexpression resulted in a significant decrease in antiviral gene expression and a significant increase in viral copy number. VHSV is a rhabdovirus, with a negative-sense and single-stranded RNA genome (Yusuff et al., 2019). MAVS is a critical immune regulator in the RLR signaling cascade and defends against RNA virus infection (Cai et al., 2015; Yoo et al., 2015). Previous studies have indicated that the RING domain of MARCH5 binds to the caspase recruitment domain (CARD) of MAVS, leading to the reduction of MAVS aggregates via proteasome-mediated degradation (Yoo et al., 2015). In addition, MARCH5 is a dual-targeting component of active RIG-I and MAVS oligomers, leading to their degradation in a proteasome-dependent manner (Park et al., 2020). This subsequently decreases the activation of downstream antiviral genes, including *tbk1*, *ifn-I*, *irf7*, and *irf3*, and results in the increase of viral replication. In concurrence with our findings, a previous study demonstrated that *MARCH*$^{+/-}$ mice and *MARCH5*-deficient immune cells showed reduced viral replication levels upon vesicular stomatitis virus infection (Yoo et al., 2015). Similarly, other MARCH proteins have also been reported to act as negative regulators of the antiviral immune response. For instance, MARCH2 plays a negative regulatory role in the NF-κB essential modulator (NEMO)-mediated signaling pathway upon viral infections (Chathuranga et al., 2020). Ectopic expression of MARCH2 in Grass carp (*Ctenopharyngodon idella*) targets TBK1 proteasomal degradation and downregulates antiviral immune responses to Poly I:C, spring viremia of carp virus (SVCV), and grass carp reovirus (GCRV) (Du et al., 2023). In zebrafish, MARCH7 and MARCH8 diminishes IFN-mediated antiviral responses by degrading the mediators of IRF3 activator (MITA) and TBK1 (Xiong et al., 2023; Zhao et al., 2022). This negative regulatory role of MARCH proteins helps to prevent excessive antiviral immune responses, playing a crucial role in maintaining cellular homeostasis during host immune defense in fish.

Recognition of pathogens via specific pathogen recognition receptors (PRR) triggers the secretion of various cytokines to regulate inflammation, recruit immune cells, activate immune cells to destroy pathogens, and promote the adaptive immune response (Torrado and Cooper, 2013). However, excessive pro-inflammatory cytokine secretion can cause various pathological conditions, including inflammatory bowel disease, psoriasis, rheumatoid arthritis, asthma, and other autoimmune disease (Sozzani et al., 2014). Previous studies have indicated that MARCH5 in mice modulates cytokine expression upon dsRNA stimulation potentially by reducing dsRNA-induced MAVS protein aggregation through MARCH5's E3 ligase activity via K48-linked polyubiquitination (Chen et al., 2017; Yan et al., 2017; Yoo et al., 2015). Similarly, other MARCH proteins, such as MARCH1 and MARCH2, negatively regulate innate inflammation by degrading IL6 receptor alpha chain, thus attenuating IL6 activity in response to bacterial endotoxins (Galbas et al., 2017). In line with this, significant downregulation of inflammatory cytokine expression was observed in macrophages overexpressing AcMARCH5 upon Poly I:C treatment, suggesting that AcMARCH5 may potentially play a role in regulating pro-inflammatory cytokine production and promoting cellular homeostasis during immune stimulation in *A. clarkii*.

Excessive oxidative stress induces mitochondrial fission, leading to cellular apoptosis. We observed enhanced cell viability and reduced apoptotic body index in FHM cells overexpressing AcMARCH5 when subjected to H_2O_2 treatment. This result was further corroborated by the reduction in the *Bax/Bcl-2* ratio increment and caspase gene expression. Bax is a pro-apoptotic protein that enhances apoptotic function and reduces tumor growth, whereas Bcl-2 is a family of proteins that prevent apoptosis by increasing mitochondrial membrane permeability (Liu et al., 2016). Analyzing the *Bax/Bcl-2* ratio provides more comprehensive information for assessing the likelihood of apoptosis than evaluating each protein individually (Oltvai et al., 1993). Caspases are a family of proteins that catalyze the cascade responsible for apoptosis (Shi, 2004). Previous studies demonstrated that caspase-3, and caspase-7 play distinct roles in intrinsic pathways during apoptosis (Brentnall et al., 2013). Another study also noted that MARCH5 ablation promotes mitochondrial fission by increasing the mitochondrial accumulation of Drp1 without altering total Drp1 levels (Wang and Poon, 2023). Overexpression of AcMARCH5 could promote the degradation of Drp1, which physically interacts with Bax during apoptosis, thereby reducing cytochrome *c* secretion critical for apoptosome formation (Wang et al., 2016). Prevention of apoptosome formation ultimately leads to the attenuation of downstream apoptotic pathways and reduced caspase expression levels. Collectively, these results suggest an anti-apoptotic role of AcMARCH5 in host cells following oxidative stress and highlight its potential involvement in apoptosis-associated diseases in *A. clarkii*.

5. Conclusion

In this study, we performed a comprehensive investigation of AcMARCH5 regarding its domain structure, tissue-specific distribution, transcriptional immune response, and functional roles using *in silico* analysis and several *in vivo/in vitro* functional assays. Our findings revealed that AcMARCH5 shares distinct structural features with

MARCH5 orthologs and exhibits ubiquitous expression in all tissues tested in healthy *A. clarkii* fish. Notably, its expression was significantly upregulated following immune stimulation with Poly I:C, LPS, or *Vibrio harveyi*. Furthermore, overexpression of AcMARCH5 in FHM cells resulted in the suppression of the RLR signaling pathway, leading to increased viral replication during VHSV infection. In addition, stimulation of Poly I:C in AcMARCH5-overexpressed RAW264.7 cells led to reduced production of proinflammatory cytokines. Moreover, AcMARCH5 demonstrated a protective effect against oxidative stressed-induced apoptosis. Collectively, these findings suggest that AcMARCH5 may play a role in modulating immune responses and maintaining cellular homeostasis during pathogenic infections and stress conditions. However, further studies are necessary to elucidate the detailed immunoregulatory mechanisms of MARCH5 in teleost species.

CRediT authorship contribution statement

B.P.M. Vileka Jayamali: Writing – original draft, Validation, Methodology, Formal analysis, Data curation, Conceptualization. **H.M. S.M. Wijerathna:** Software, Methodology, Data curation. **D.M.K.P. Sirisena:** Software, Methodology, Data curation. **H.A.C.R. Hanchapola:** Methodology, Investigation. **W.A.D.L.R. Warnakula:** Methodology, Investigation, Data curation. **U.P.E. Arachchi:** Methodology, Investigation. **D.S. Liyanage:** Writing – review & editing. **Sumi Jung:** Methodology, Investigation. **Qiang Wan:** Writing – review & editing, Supervision, Data curation, Conceptualization. **Jehee Lee:** Writing – review & editing, Supervision, Resources, Project administration.

Acknowledgement

This study was supported by the Basic Science Research Program of the National Research Foundation of Korea (NRF) and was funded by the Ministry of Education (2019R1A6A1A03033553), the Korea Institute of Marine Science and Technology Promotion (KIMST), and the Ministry of Oceans and Fisheries (RS-2022-KS221670).

Appendix A. Supplementary data

Supplementary data to this article can be found online at https://doi.org/10.1016/j.dci.2024.105283.

Data availability

Data will be made available on request.

References

Akira, S., 2003. Toll-like receptor signaling. J. Biol. Chem. 278 (40), 38105–38108. https://doi.org/10.1074/jbc.R300028200.

Bartee, E., Mansouri, M., Nerenberg, B.T.H., Gouveia, K., Fru, K., 2004. Downregulation of major histocompatibility complex class I by human downregulation of major histocompatibility complex class I by human ubiquitin ligases related to viral immune evasion proteins. J. Virol. 78 (3), 1109–1120. https://doi.org/10.1128/JVI.78.3.1109.

Bauer, J., Bakke, O., Morth, J.P., 2017. Overview of the membrane-associated RING-CH (MARCH) E3 ligase family. New Biotechnology 38, 7–15. https://doi.org/10.1016/j.nbt.2016.12.002.

Bond, S.T., Moody, S.C., Liu, Y., Civelek, M., Villanueva, C.J., Gregorevic, P., Kingwell, B. A., Hevener, A.L., Lusis, A.J., Henstridge, D.C., Calkin, A.C., Drew, B.G., 2018. The E3 ligase MARCH5 is a PPARγ target gene that regulates mitochondria and metabolism in adipocytes. Endocrinology and Metabolism 316 (2), 293–304. https://doi.org/10.1152/ajpendo.00394.2018.

Brentnall, M., Rodriguez-Menocal, L., De Guevara, R.L., Cepero, E., Boise, L.H., 2013. Caspase-9, caspase-3 and caspase-7 have distinct roles during intrinsic apoptosis. BMC Cell Biol. 14 (1). https://doi.org/10.1186/1471-2121-14-32.

Cai, X., Chen, J., Xu, H., Liu, S., Jiang, Q.-X., Halfmann, R., Chen, Z.J., 2015. Prion-like polymerization underlies signal transduction in antiviral immune defense and inflammasome activation. Cell 156 (6), 1207–1222. https://doi.org/10.1016/j.cell.2014.01.063.Prion-like.

Chathuranga, K., Kim, T., Lee, H., Park, J., Kim, J., Chathuranga, W.A.G., Ekanayaka, P., Choi, Y.J., Lee, C., Kim, C., Jung, J.U., Lee, J., 2020. Negative regulation of NEMO signaling by the ubiquitin E3 ligase MARCH2. EMBO J. 39 (21). https://doi.org/10.15252/embj.2020105139.

Chen, N., Xia, P., Li, S., Zhang, T., Wang, T.T., Zhu, J., 2017. RNA sensors of the innate immune system and their detection of pathogens. IUBMB Life 69 (5), 297–304. https://doi.org/10.1002/iub.1625.

Cheng, M.C., See, M.S., Wang, P.C., Kuo, Y.T., Ho, Y.S., Chen, S.C., Tsai, M.A., 2022. Lymphocystis disease virus infection in clownfish Amphiprion ocellaris and Amphiprion clarkii in taiwan. Animals 13 (1), 1–12. https://doi.org/10.3390/ani13010153.

Chu, P.Y., Tzeng, Y.D.T., Chiu, Y.H., Lin, H.Y., Kuo, C.H., Hou, M.F., Li, C.J., 2021. Multi-omics reveals the immunological role and prognostic potential of mitochondrial ubiquitin ligase MARCH5 in human breast cancer. Biomedicines 9 (10), 1329. https://doi.org/10.3390/biomedicines9101329.

Dahle, M.K., Wessel, Ø., Timmerhaus, G., Nyman, I.B., Jørgensen, S.M., Rimstad, E., Krasnov, A., 2015. Transcriptome analyses of Atlantic salmon (Salmo salar L.) erythrocytes infected with piscine orthoreovirus (PRV). Fish Shellfish Immunol. 45 (2), 780–790. https://doi.org/10.1016/j.fsi.2015.05.049.

DeLano, W.L., 2002. PyMOL: an open-source molecular graphics tool. CCP4 NEWSLETTER ON PROTEIN CRYSTALLOGRAPHY 40, 82–92.

Deshaies, R.J., Joazeiro, C.A.P., 2009. RING domain E3 ubiquitin ligases. Annu. Rev. Biochem. 78, 399–434. https://doi.org/10.1146/annurev.biochem.78.101807.093809.

Du, J., Xiao, H., Hu, Y., Li, Z., 2023. march2 negatively regulates antiviral immune response by targeting tbk1 in grass carp (Ctenopharyngodon idella). Fish Shellfish Immunol. 140, 108965. https://doi.org/10.1016/j.fsi.2023.108965.

Fortier, M., Kent, S., Ashdown, H., Poole, S., Boksa, P., Luheshi, G.N., Kent, S., Ashdown, H., Boksa, P., Luheshi, G.N., 2023. The viral mimic, polyinosinic: polycytidylic acid, induces fever in rats via an interleukin-1-dependent mechanism. American journal of physiology 287 (4), 759–766. https://doi.org/10.1152/ajpregu.00293.2004.

Frost, R.A., Lang, C.H., 2008. Regulation of muscle growth by pathogen-associated molecules. J. Anim. Sci. 86 (14), 84–93. https://doi.org/10.2527/jas.2007-0483.

Fukuda, H., Nakamura, N., Hirose, S., 2006. MARCH-III Is a novel component of Endosomes with properties similar to those of MARCH-II. The journal of biochemistry 139 (1), 137–145. https://doi.org/10.1093/jb/mvj012.

Galbas, T., Raymond, M., Sabourin, A., Bourgeois-Daigneault, M.-C., Guimont-Desrochers, F., Yun, T.J., Cailhier, J.-F., Ishido, S., Lesage, S., Cheong, C., Thibodeau, J., 2017. MARCH1 E3 ubiquitin ligase dampens the innate inflammatory response by modulating monocyte functions in mice. J. Immunol. 198 (2), 852–861. https://doi.org/10.4049/jimmunol.1601168.

Goto, E., Satoshi, Ishido, Sato, Y., Ohgimoto, S., Ohgimoto, K., Nagano-Fujii, M., Hotta, H., 2003. c-MIR, a human E3 ubiquitin ligase, is a functional homolog of herpesvirus proteins MIR1 and MIR2 and has similar activity. J. Biol. Chem. 278 (17), 14657–14668. https://doi.org/10.1074/jbc.M211285200.

Gu, H., Li, Q., Huang, S., Lu, W., Cheng, F., Gao, P., Wang, C., Miao, L., Mei, Y., Wu, M., 2015. Mitochondrial E3 ligase March5 maintains stemness of mouse ES cells via suppression of ERK signalling. Nat. Commun. 6 (1), 7112. https://doi.org/10.1038/ncomms8112.

Hallgren, J., Tsirigos, K.D., Pedersen, M.D., Armenteros, J.J.A., Marcatili, P., Nielsen, H., Krogh, A., Winther, O., 2022. DeepTMHMM predicts alpha and beta transmembrane proteins using deep neural networks. bioRxiv. https://doi.org/10.1101/2022.04.08.487609.

Haschka, M.D., Karbon, G., Soratroi, C., O'Neill, K.L., Luo, X., Villunger, A., 2020. MARCH5-dependent degradation of MCL1/NOXA complexes defines susceptibility to antimitotic drug treatment. Cell Death Differ. 27, 2297–2312. https://doi.org/10.1038/s41418-020-0503-6.

Hassink, G., Kikkert, M., Voorden, S. Van, Lee, S., Spaapen, R., Laar, T. Van, Coleman, C. S., Bartee, E., Fruh, K., Chau, V., Wiertz, E., 2005. TEB4 is a C4HC3 RING finger-containing ubiquitin ligase of the endoplasmic reticulum. Biochem. J. 388 (2), 647–655. https://doi.org/10.1042/BJ20041241.

Hirose, Y., 1995. Patterns of pair formation in protandrous anemonefishes,Amphiprion clarkii, A. frenatus andA. perideraion, on coral reefs of Okinawa, Japan. Environ. Biol. Fish. 43 (2), 153–161. https://doi.org/10.1007/BF00002485.

Iyengar, P.V., Hirota, T., Hirose, S., Nakamura, N., 2011. Membrane-associated RING-CH 10 (MARCH10 protein) is a microtubule-associated E3 ubiquitin ligase of the spermatid flagella. J. Biol. Chem. 286 (45), 39082–39090. https://doi.org/10.1074/jbc.M111.256875.

Jabbour, M., Campbell, E.M., Fares, H., Lybarger, L., 2009. Discrete domains of MARCH1 mediate its localization, functional interactions, and posttranscriptional control of expression. J. Immunol. 183 (10), 6500–6512. https://doi.org/10.4049/jimmunol.0901521.

Jiang, W.D., Zhang, L., Feng, L., Wu, P., Liu, Y., Jiang, J., Kuang, S.Y., Tang, L., Zhou, X. Q., 2020. Inconsistently impairment of immune function and structural integrity of head kidney and spleen by vitamin A deficiency in grass carp (Ctenopharyngodon idella). Fish Shellfish Immunol. 99 (October 2019), 243–256. https://doi.org/10.1016/j.fsi.2020.02.019.

Karbowski, M., Neutzner, A., Youle, R.J., 2007. The mitochondrial E3 ubiquitin ligase MARCH5 is required for Drp1 dependent mitochondrial division. JCB (J. Cell Biol.) 178 (1), 71–84. https://doi.org/10.1083/jcb.200611064.

Kim, G., Sohn, H., Omeka, W.K.M., Lim, C., Elvitigala, D.A.S., Lee, J., 2023. Functional characterization and expression analysis of c-type and g-like-type lysozymes in yellowtail clownfish (Amphiprion clarkii). Fisheries and Aquatic Sciences 26 (3), 188–203. https://doi.org/10.47853/FAS.2023.e16.

Kim, J.O., Kim, W.S., Kim, S.W., Han, H.J., Kim, J.W., Park, M.A., Oh, M.J., 2014. Development and application of quantitative detection method for viral hemorrhagic

septicemia virus (VHSV) genogroup IVa. Viruses 6 (5), 2204–2213. https://doi.org/10.3390/v6052204.
Kim, S., Park, Y., Yoo, Y., Cho, H., 2016. Self-clearance mechanism of mitochondrial E3 ligase MARCH5 contributes to mitochondria quality control. FEBS J. 283 (2), 294–304. https://doi.org/10.1111/febs.13568.
Lam, H.S., Hue, N.T.N., 2021. Common diseases in clownfish : a review. Vietnam Journal of Marine Science and Technology 21 (4A), 129–143. https://doi.org/10.15625/1859-3097/16611.
Lei, W., Li, J., Li, C., Chen, L., Huang, F., Xiao, D., Zhang, J., Zhao, J., Li, G., Qu, T., Zhou, H., Liao, Y., Chen, M., 2021. MARCH5 restores endothelial cell function against ischaemic/hypoxia injury via Akt/eNOS pathway. J. Cell Mol. Med. 25 (7), 3182–3193. https://doi.org/10.1111/jcmm.16386.
Lin, H., Li, S., Shu, H., 2019. The membrane-associated MARCH E3 ligase family: emerging roles in immune regulation. Front. Immunol. 10, 1–10. https://doi.org/10.3389/fimmu.2019.01751.
Liu, Z., Ding, Y., Ye, N., Wild, C., Chen, H., Zhou, J., 2016. Direct activation of Bax protein for cancer therapy. Med. Res. Rev. 36 (2), 313–341. https://doi.org/10.1002/med.21379.Direct.
Livak, K.J., Schmittgen, T.D., 2001. Analysis of relative gene expression data using real-time quantitative PCR and the 2-ΔΔCT method. Methods 25 (4), 402–408. https://doi.org/10.1006/meth.2001.1262.
Lu, Y.C., Yeh, W.C., Ohashi, P.S., 2008. LPS/TLR4 signal transduction pathway. Cytokine 42 (2), 145–151. https://doi.org/10.1016/j.cyto.2008.01.006.
Madeira, F., Pearce, M., Tivey, A.R.N., Basutkar, P., Lee, J., Edbali, O., Madhusoodanan, N., Kolesnikov, A., Lopez, R., 2022. Search and sequence analysis tools services from EMBL-EBI in 2022. Nucleic Acids Res. 50 (1), 276–279. https://doi.org/10.1093/nar/gkac240.
Marchler-bauer, A., Bo, Y., Han, L., He, J., Lanczycki, C.J., Lu, S., Chitsaz, F., Derbyshire, M.K., Geer, R.C., Gonzales, N.R., Gwadz, M., Hurwitz, D.I., Lu, F., Marchler, G.H., Song, J.S., Thanki, N., Wang, Z., Yamashita, R.A., Zhang, D., et al., 2017. CDD/SPARCLE: functional classification of proteins via subfamily domain architectures. Nucleic Acids Res. 45 (1), 200–203. https://doi.org/10.1093/nar/gkw1129.
Marchler-bauer, A., Derbyshire, M.K., Gonzales, N.R., Lu, S., Chitsaz, F., Geer, L.Y., Geer, R.C., He, J., Gwadz, M., Hurwitz, D.I., Lanczycki, C.J., Lu, F., Marchler, G.H., Song, J.S., Thanki, N., Wang, Z., Yamashita, R.A., Zhang, D., Zheng, C., Bryant, S.H., 2015. CDD: NCBI's conserved domain database. Nucleic Acids Res. 43 (D1), 222–226. https://doi.org/10.1093/nar/gku1221.
Marudhupandi, T., Kumar, T.T.A., Prakash, S., Balamurugan, J., Dhayanithi, N.B., 2017. Vibrio parahaemolyticus a causative bacterium for tail rot disease in ornamental fish, Amphiprion sebae. Aquaculture Reports 8 (October), 39–44. https://doi.org/10.1016/j.aqrep.2017.09.004.
Morokuma, Y., Nakamura, N., Kato, A., Notoya, M., Yamamoto, Y., Sakai, Y., Fukuda, H., Yamashina, S., Hirata, Y., Hirose, S., 2007. MARCH-XI, a novel transmembrane ubiquitin ligase implicated in ubiquitin-dependent protein sorting in developing spermatids. Journal of Biological Chemistryemistry 282 (34), 24806–24815. https://doi.org/10.1074/jbc.M700414200.
Nagashima, S., Tokuyama, T., Yonashiro, R., Inatome, R., Yanagi, S., 2014. Roles of mitochondrial ubiquitin ligase MITOL/MARCH5 in mitochondrial dynamics and diseases. J. Biochem. 155 (5), 273–279. https://doi.org/10.1093/jb/mvu016.
Nakamura, N., Fukuda, H., Kato, A., Hirose, S., 2005. MARCH-II is a syntaxin-6 – binding protein involved in endosomal trafficking. Mol. Biol. Cell 16 (4), 1696–1710. https://doi.org/10.1091/mbc.E04.
Nakamura, N., Kimura, Y., Tokuda, M., Honda, S., Hirose, S., 2006. MARCH-V is a novel mitofusin 2- and Drp1-binding protein able to change mitochondrial morphology. EMBO Rep. 7 (10), 1019–1022. https://doi.org/10.1038/sj.embor.7400790.
Oltvai, Z.N., Milkman, C.L., Korsmeyer, S.J., 1993. Bcl-2 heterodimerizes in vivo with a conserved homolog, Bax, that accelerates programmed cell death. Cell Press 74 (4), 609–619. https://doi.org/10.1016/0092-8674(93)90509-o.
Ou, M., Huang, R., Xiong, L., Luo, L., Chen, G., Liao, L., Li, Y., He, L., Zhu, Z., Wang, Y., 2017. Molecular cloning of the MARCH family in grass carp (Ctenopharyngodon idellus) and their response to grass carp reovirus challenge. Fish Shellfish Immunol. 63, 480–490. https://doi.org/10.1016/j.fsi.2017.02.030.
Owczarzy, R., Tataurov, A.V., Wu, Y., Manthey, J.A., Mcquisten, K.A., Almabrazi, H.G., Pedersen, K.F., Lin, Y., Garretson, J., Mcentaggart, N.O., Sailor, C.A., Dawson, R.B., Peek, A.S., 2008. IDT SciTools: a suite for analysis and design of nucleic acid oligomers. Nucleic Acids Res. 36 (2), 163–169. https://doi.org/10.1093/nar/gkn198.
Park, Y.-Y., Nguyen, O.T.K., Kang, H., Cho, H., 2014. MARCH5-mediated quality control on acetylated Mfn1 facilitates mitochondrial homeostasis and cell survival. Cell Death $ Disease 5, 1172. https://doi.org/10.1038/cddis.2014.142.
Park, Y., Oanh, N.T.K., Heo, J., Kim, S., Lee, H., Lee, H., Lee, J.-H., Kang, H.C., Lim, W., Yoo, Y.-S., Cho, H., 2020. Dual targeting of RIG-I and MAVS by MARCH5 mitochondria ubiquitin ligase in innate immunity. Cell. Signal. 67, 109520. https://doi.org/10.1016/j.cellsig.2019.109520.
Passantino, L., Altamura, M., Cianciotta, A., Patruno, R., Tafaro, A., Jirillo, E., Passantino, G.F., 2002. Fish immunology. I. Binding and engulfment of Candida albicans by erythrocytes of rainbow trout (Salmo gairdneri Richardson). Immunopharmacol. Immunotoxicol. 24 (4), 665–678. https://doi.org/10.1081/iph-120016050.
Qin, L., Xi, S., 2022. The role of mitochondrial fission proteins in mitochondrial dynamics in kidney disease. International Journal of Molecular Science 23 (23), 14725. https://doi.org/10.3390/ijms232314725.
Rebl, A., Köbis, J.M., Fischer, U., Takizawa, F., Verleih, M., Wimmers, K., Goldammer, T., 2011. MARCH5 gene is duplicated in rainbow trout, but only fish-specific gene copy is up-regulated after VHSV infection. Fish & Shellfish Immunology journal 31 (6), 1041–1050. https://doi.org/10.1016/j.fsi.2011.09.004.
Ren, J., Wen, L., Gao, X., Jin, C., Xue, Y., Yao, X., 2009. Dog 1.0: illustrator of protein domain structures. Cell Res. 19 (2009.6), 271–273. https://doi.org/10.1038/cr.
Rice, P., Longden, L., Bleasby, A., 2000. EMBOSS: the European molecular biology open software suite. Trends Genet. 16 (6), 276–277. https://doi.org/10.1016/S0168-9525(00)02024-2.
Rigotti, F.D.A., Gassart, A. De, Pforr, C., Cano, F., Guessan, P.N., Combes, A., Camossetto, V., Lehner, P.J., Pierre, P., Gatti, E., 2017. MARCH9-mediated ubiquitination regulates MHC I export from the TGN. Immunol. Cell Biol. 95 (9), 753–764. https://doi.org/10.1038/icb.2017.44.
Shanaka, K.A.S.N., Madushani, K.P., Madusanka, R.K., Neranjan Tharuka, M.D., Sellaththurai, S., Yang, H., Jung, S., Lee, J., 2021. Fish and Shellfish Immunology Transcription profile, NF- κB promoter activation, and antiviral activity of Amphiprion clarkii Akirin-2. Fish Shellfish Immunol. 108, 14–23. https://doi.org/10.1016/j.fsi.2020.11.018.
Shi, H.-X., Liu, X., Wang, Q., Tang, P.P., Liu, X.Y., Shan, Y.F., Wang, C., 2011. Mitochondrial ubiquitin ligase MARCH5 promotes TLR7 signaling by attenuating TANK action. PLoS Pathog. 7 (5), 1002057. https://doi.org/10.1371/journal.ppat.1002057.
Shi, Y., 2004. Caspase activation, inhibition, and reactivation: a mechanistic view. Protein Sci. 13 (8), 1979–1987. https://doi.org/10.1110/ps.04789804.Protein.
Sievers, F., Higgins, D.G., 2017. Clustal Omega for making accurate alignments of many protein sequences. The Protein Society 27 (1), 135–145. https://doi.org/10.1002/pro.3290.
Sozzani, S., Abbracchio, M.P., Annese, V., Danese, S., Pità, O. De, Sarro, G. De, Maione, S., Olivieri, I., Parodi, A., Sarzi-Puttini, P., 2014. Chronic inflammatory diseases: do immunological patterns drive the choice of biotechnology drugs? A critical review. Autoimmunity 47 (5), 287–306. doi:10.3109/08916934.2014.897333.
Tamura, K., Stecher, G., Kumar, S., 2021. MEGA11: molecular evolutionary genetics analysis version 11. Mol. Biol. Evol. 38 (7), 3022–3027. https://doi.org/10.1093/molbev/msab120.
Torrado, E., Cooper, A.M., 2013. Cytokines in the balance of protection and pathology during mycobacterial infections. The new paradigm of immunity to tuberculosis 783, 121–140. https://doi.org/10.1007/978-1-4614-6111-1.
Wang, J., Aung, L.H.H., Prabhakar, B.S., Li, P., 2016. The mitochondrial ubiquitin ligase plays an anti-apoptotic role in cardiomyocytes by regulating mitochondrial fission. J. Cell Mol. Med. 20 (12), 2278–2288. https://doi.org/10.1111/jcmm.12914.
Wang, Y., Poon, R.Y.C., 2023. MARCH5 regulates mitotic apoptosis through MCL1-dependent and independent mechanisms. Cell Death Differ. 30 (3), 753–765. https://doi.org/10.1038/s41418-022-01080-2.
Wijerathna, H.M.S.M., Nadarajapillai, K., Udayantha, H.M.V., Kasthuriarachchi, T.D.W., Shanaka, K.A.S.N., Kwon, H., Wan, Q., Lee, J., 2022. Molecular delineation, expression profiling, immune response, and anti-apoptotic function of a novel clusterin homolog from big-belly seahorse (Hippocampus abdominalis). Fish Shellfish Immunol. 124, 289–299. https://doi.org/10.1016/j.fsi.2022.04.015.
Xiong, S., Ying, Y., Long, Z., Li, J., Zhang, Y., 2023. Zebrafish MARCH7 negatively regulates IFN antiviral response by degrading TBK1. Int. J. Biol. Macromol. 240, 124384. https://doi.org/10.1016/j.ijbiomac.2023.124384.
Xu, S., Cherok, E., Das, S., Li, S., Roelofs, B.A., Ge, S.X., Polster, B.M., Boyman, L., Lederer, W.J., Wang, C., Karbowski, M., 2016. Mitochondrial E3 ubiquitin ligase MARCH5 controls mitochondrial fission and cell sensitivity to stress-induced apoptosis through regulation of MiD49 protein. Mol. Biol. Cell 27 (2), 349–359. https://doi.org/10.1091/mbc.E15-09-0678.
Yan, B., Zhou, L., Hu, M., Li, M., Lin, H., Yang, Y., Wang, Y.-Y., Shu, H., 2017. PKACs attenuate innate antiviral response by phosphorylating VISA and priming it for MARCH5-mediated degradation. PLoS Pathog. 13 (9). https://doi.org/10.1371/journal.ppat.1006648.
Yonashiro, R., Ishido, S., Kyo, S., Fukuda, T., Goto, E., Matsuki, Y., Ohmura-Hoshino, M., Sada, K., Hotta, H., Yamamura, H., Inatome, R., Yanagi, S., 2006. A novel mitochondrial ubiquitin ligase plays a critical role in mitochondrial dynamics. EMBO J. 25 (15), 3618–3626. https://doi.org/10.1038/sj.emboj.7601249.
Yoo, Y., Park, Y., Kim, J., Cho, H., Kim, S., Lee, H., Kim, T., Kim, Y.S., Lee, Y., Kim, C., Jung, J.U., Lee, J., Cho, H., 2015. The mitochondrial ubiquitin ligase MARCH5 resolves MAVS aggregates during antiviral signalling. Nat. Commun. 6 (7910), 1–14. https://doi.org/10.1038/ncomms8910.
Yoo, Y., Park, Y., Lee, H., Oanh, N.T.K., Cho, M., Heo, J., Lee, E., Cho, H., Park, Y., Cho, H., 2019. Mitochondria ubiquitin ligase, MARCH5 resolves hepatitis B virus X protein aggregates in the liver pathogenesis. Cell Death Dis. 10 (12). https://doi.org/10.1038/s41419-019-2175-z.
Yusuff, S., Kurath, G., Kim, M.S., Tesfaye, T.M., Li, J., Mckenney, D.G., Vakharia, V.N., 2019. The glycoprotein, non-virion protein, and polymerase of viral hemorrhagic septicemia virus are not determinants of host-specific virulence in rainbow trout. Virol. J. 16 (31). https://doi.org/10.1186/s12985-019-1139-3.
Zhang, X., He, X., Austin, B., 2020. Vibrio harveyi: a serious pathogen of fish and invertebrates in mariculture. Marine Life Science & Technology 2 (3), 231–245. https://doi.org/10.1007/s42995-020-00037-z.
Zhang, Yang, 2008. I-TASSER server for protein 3D structure prediction. BMC Bioinf. 9 (1), 40. https://doi.org/10.1186/1471-2105-9-40.
Zhang, Yanzhao, Tada, T., Ozono, S., Yao, W., Tanaka, M., Yamaoka, S., Kishigami, S., Fujita, H., Tokunaga, K., 2019. Membrane-associated RING-CH (MARCH) 1 and 2

are MARCH family members that inhibit HIV-1 infection. J. Biol. Chem. 294 (10), 3397–3405. https://doi.org/10.1074/jbc.AC118.005907.
Zhao, X., Dan, C., Gong, X., Li, Y., Qu, Z., Sun, H., 2022. Zebrafish MARCH8 downregulates fish IFN response by targeting MITA and TBK1 for protein degradation. Dev. Comp. Immunol. 135. https://doi.org/10.1016/j.dci.2022.104485.
Zheng, C., Tang, Y.D., 2021. When MARCH family proteins meet viral infections. Virol. J. 18 (49), 1–5. https://doi.org/10.1186/s12985-021-01520-4.